Summer 2005

Maneuvering Control of a Spacecraft with Propellant Sloshing

Philip A. Savella
Embry-Riddle Aeronautical University - Daytona Beach

MANEUVERING CONTROL OF A SPACECRAFT WITH PROPELLANT SLOSHING

By

Philip A. Savella

A thesis submitted to the Physical Sciences Department

In Partial Fulfillment of the Requirements of

Master of Science in Space Science

Embry-Riddle Aeronautical University

Daytona Beach, FL 32114

Summer 2005

MANEUVERING CONTROL OF A SPACECRAFT WITH PROPELLANT SLOSHING

By Philip A. Savella

This thesis was prepared under the direction of the candidate's thesis committee chair, Dr. Mahmut Reyhanoglu, Department of Physical Sciences, and has been approved by the members of his thesis committee. It was submitted to the Department of Physical Sciences and was accepted in partial fulfillment of the requirements for the

Degree of

Master of Science in Space Sciences

THESIS COMMITTEE:

M. Reyhanoglu
Dr. Mahmut Reyhanoglu, Chair

Dr. Bereket Berhane, Member

M. Hickey
Dr. Michael Hickey, Member

MSSPS Graduate Program Coordinator

Department Chair, Physical Sciences

Associate Chancellor, Daytona Beach Campus

8/10/05
Date

Acknowledgments

First and foremost, I would like to thank my advisor, Dr. Mahmut Reyhanoglu, for his infinite patience in bestowing on me what I am sure is only a small part of his knowledge on this subject. Only with his counsel did this thesis achieve its *desired state*.

Thanks to my parents, Deborah and Italo, and my sweetheart Jen for their perpetual pipeline of love and psychological upkeep.

Finally, I would like to dedicate this work to the late Kenneth Lloyd Myers, whose perseverance in all endeavors was an inspiration.

Abstract

Propellant slosh has been a problem studied in spacecraft design since the early days of large, liquid-fuel rockets. The conventional design solution involves physical structures inside the fuel tanks that limit propellant motion. Although effective, baffles and bladders add to spacecraft mass and structural complexity. In this research, the sloshing fuel mass is treated as an unactuated degree of freedom within a rigid body. Specifically, the propellant is modeled as a pendulum mass anchored at the center of a spherical tank. After obtaining the coupled equations of motion, several linear controllers are developed to achieve planar spacecraft pitch-maneuvers while suppressing the slosh mode. The performance of these linear controllers will be compared to that of a nonlinear controller developed using Lyapunov's Second Method. It is shown that the linear controllers are ill-equipped to achieve the desired spacecraft attitude and transverse velocity simultaneously, especially during aggressive pitch-maneuvers; while the Lyapunov controller is superior in this regard.

Contents

List of Figures

List of Tables

Chapter 1

Introduction

1.1 Propellant Sloshing Problem

In April of 1957, a Jupiter Intermediate Range Ballistic Missile was terminated 90 seconds after launch due to propellant slosh. Ever since the launch of the early high-efficiency rockets, controlling liquid fuel slosh within a launch vehicle has been a major design concern. Moreover, with today's large and complex spacecraft, a substantial mass of fuel is necessary to place them into orbit and to perform orbital maneuvers. The mass of fuel contained in the tanks of a geosynchronous satellite amounts to approximately 40% of its total mass [1]. When the fuel tanks are only partially filled, large quantities of fuel move inside the tanks under translational and rotational accelerations and generate the slosh dynamics.

The traditional treatment of liquid slosh control began with the inclusion of physical barriers, such as baffles and complete compartmentalization (Figure 1.1), meant to limit the movement of liquid fuel to small amplitudes of high, negligible frequencies. Later, bladders were added to the list of ways to limit these motions (Figure 1.2). These suppression methods involve adding to the spacecraft structural mass,

thereby increasing mission cost.

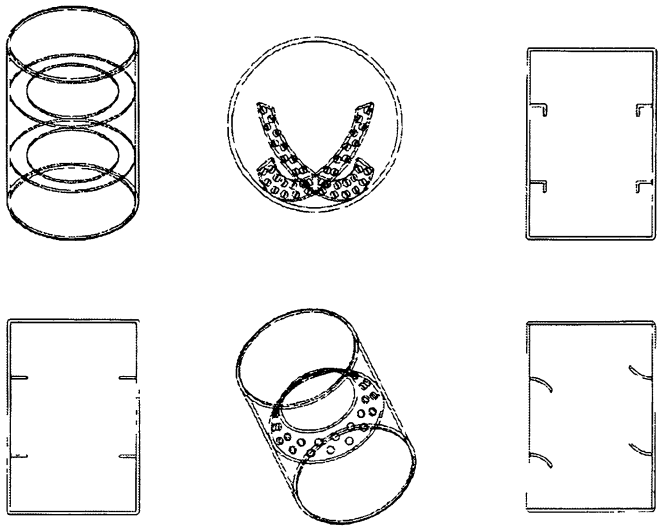

Figure 1.1: Common baffle types.

The NASA document on space vehicle design [2] discusses the slosh suppression problem and criteria formulated as of May 1969. Featured suppression devices in [2] are rigid-ring baffles, cruciform baffles, deflectors, flexible ring baffles, floating cans, positive-expulsion bags, and diaphragms. The document presents methods to estimate the amount of damping provided by each suppression device. Different tank geometries including cylindrical, spherical, and toroidal geometries and tank compartmentalization issues are treated in detail. Both low gravity and zero gravity slosh suppression are discussed.

The work in Biswal et al [3] studies the effects of baffle positions (and quantities) on sloshing frequency, as well as tanks containing no baffles. Tanks are rectangular in two dimensions using rigid rectangular plates to suppress fluid motion. Mathematical technique includes use of the velocity potential function solved using finite-element analysis. Results show baffles are more effective when near the free-surface of the fluid. Venugopal and Bernstein in [4] consider active control mechanisms for controlling

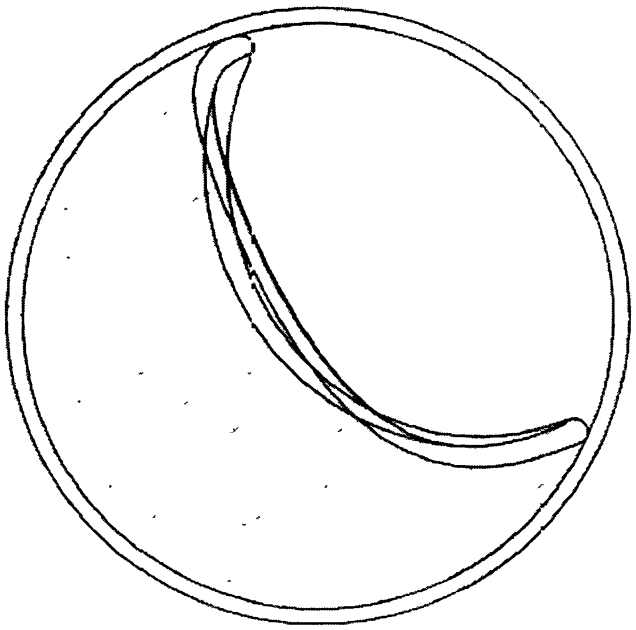

Figure 1.2: Fuel bladder.

slosh in rectangular tanks. Two methods are used: surface pressure control (speaker) and surface flap actuation. Fluid is assumed to be incompressible, inviscid, and irrotational, and feedback controllers are designed using a Linear-Quadratic-Gaussian (LQG) synthesis. Experimental results show steady-state slosh amplitude lower than the no-actuator case.

The effect of liquid fuel slosh on spinning spacecraft has been studied by Hubert in [5] and [6]. In [5], different slosh motion types - surface waves, bulk fluid motion, and vortices as well as fluid configurations during spinning are defined. In [6], the design and flight performance of a system is studied for rapid attitude maneuvers by a spinning vehicle. Control strategies for launch vehicles with propellant sloshing have been studied extensively in the literature. Blackburn and Vaughan in [7] develop an advanced linear model of the Saturn V launch vehicle and apply linear optimal control and filtering theory to control the vehicle. Freudenberg and Morton in [8] study the

problem of robust control of a launch vehicle subject to aerodynamic, flexible, and slosh mode instabilities.

It has been demonstrated in [9] that pendulum and mass-spring models can approximate complicated fluid and structural dynamics; such models have formed the basis for many studies on dynamics and control of space vehicles with fuel slosh. For accelerating space vehicles, several thrust vector control design approaches have been developed to suppress the fuel slosh dynamics. These approaches have commonly employed methods of linear control design ([1], [10], [11]) and adaptive control [12]. A number of related papers, following a similar approach, are motivated by robotic systems moving liquid filled containers ([13], [14], [15], [16], [17]. [18], [19], [20]). In most of these approaches, suppression of the slosh dynamics inevitably leads to excitation of the transverse vehicle motion through coupling effects; this is a major drawback which has not been adequately addressed in the published literature.

Kim and Choi in [21] consider the problem of launch vehicle control using a pendulum model that includes the sloshing pendulum on top of a fixed mass of non-sloshing fuel. The stability of the slosh mode is analyzed, and an attitude controller is designed for both the stable and unstable slosh mode case. Simulation results show that a proportional-plus-derivative (PD) controller that includes a slosh filter performs reasonably well in both the open-loop and closed-loop cases.

In this thesis a spacecraft with a partially filled spherical fuel tank is considered and the lowest frequency slosh mode is included in the dynamic model using the common pendulum analogy. Although present in the actual system, the higher frequency slosh modes are assumed to be small in this approach. A complete set of spacecraft control forces and moments is assumed to be available to accomplish planar maneuvers. Aerodynamic effects are ignored here, although they can be easily included in the spacecraft dynamics assuming that they are cancelled by the spacecraft con-

trols. It is also assumed that the spacecraft is in a zero gravity environment, but this assumption is for convenience only. These simplifying assumptions render the problem tractable, while still reflecting the important coupling between the unactuated slosh dynamics and the actuated rigid body motion of the spacecraft. The control objective, as is typical for spacecraft orbital maneuvering problems, is to control the translational velocity vector and the attitude of the spacecraft, while attenuating the slosh mode. Subsequently, a mathematical model that reflects all of these assumptions is constructed. Finally, both linearization-based controllers and Lyapunov-based nonlinear feedback controllers are designed to achieve this control objective.

1.2 Contribution of Thesis

This thesis presents a useful comparison of state-of-the-art linear and nonlinear control designs for a spacecraft with propellant sloshing. The contribution of this thesis can be summarized as follows:

- Development of mathematical models using various control configurations.
- Design of linearization-based controllers (filtered PD controllers and LQR controllers) using only a torquer.
- Design of linearization-based controllers (filtered PD controllers and LQR controllers) using only a side thruster.
- Design of switched-feedback controllers using both a torquer and a side thruster.
- Design of a Lyapunov-based nonlinear feedback controller using both a torquer and a side thruster.

1.3 Organization of Thesis

The content of this thesis following this introduction begins in Chapter 2 with a review of the background mathematics found in modern control theory. The chapter begins with the development of the mathematical model specific to the spacecraft fuel slosh problem, followed by linearization of the equations of motion under small amplitude assumptions. Important concepts visited include the interpretation of block diagrams, transfer functions, modeling in state space, and finally common controller types (especially proportional-plus-derivative controllers).

Chapter 3 applies linear controller types of varying complexity and performance characteristics to the slosh model. Beginning with a generalized filter to suppress the slosh dynamics, control is attempted with an onboard torquer, then with side-thrusters, and then with both actuators in sequence. This is next compared to LQR based controllers acting on the same actuator combinations. These methods require the linearization of the equations of motion.

Chapter 4 introduces Lyapunov's Second Method (L2M) for the treatment of the equations of motion including their non-linearities. This is the method that will be favored in the treatment of more sophisticated models as it is expected that L2M will perform well on all state variables and for any drastic initial conditions.

Chapter 5 summarizes the results produced for all controller types discussed, and conclusions and suggestions for future work are presented in Chapter 6.

Chapter 2

Mathematical Model

2.1 Introduction

This chapter presents the spacecraft model used in the development of the control systems studied in this research. First, the equations of motion are formulated for the underactuated propellant slosh problem. These equations are then linearized in preparation for the development of linear controllers in Chapter 3. Once simplified, it is shown that the model behaves as a second-order system, allowing for the identification of certain system characteristics. System visualization and manipulation techniques are reviewed in a discussion of block diagrams, transfer functions, and finally state space representation.

2.2 Pendulum Model

In this section, we formulate the dynamics of a spacecraft with a spherical fuel tank and include the lowest frequency slosh mode. We represent the spacecraft as a rigid body (base body) and the sloshing fuel mass as an internal body, and follow the

development in [22] to express the equations of motion in terms of the spacecraft translational velocity vector, the attitude angle, the angular velocity, the internal (shape) coordinate representing the slosh mode, and its derivative.

To summarize the formulation in [22], let $v \in \mathbf{R}^3$, $\omega \in \mathbf{R}^3$, and $\xi \in \mathbf{R}$ denote the base body translational velocity vector, the base body angular velocity vector, and the internal coordinate, respectively. In these coordinates, the Lagrangian has the form $L = L(v, \omega, \xi, \dot{\xi})$, which is $SE(3)$-invariant in the sense that it does not depend on the base body position and attitude. The generalized forces and moments on the spacecraft are assumed to consist of control inputs which can be partitioned into two parts: $\tau_t \in \mathbf{R}^{n_t}$ (typically from thrusters) is the vector of generalized forces that act on the base body and $\tau_r \in \mathbf{R}^{n_r}$ (typically from symmetric rotors, reaction wheels, and thrusters) is the vector of generalized torques that act on the base body. We also assume that the internal dissipative forces are derivable from a Rayleigh dissipation function R. Then, the equations of motion of the spacecraft with internal dynamics are shown in [23] to be given by:

$$\frac{d}{dt}\frac{\partial L}{\partial v} + \hat{\omega}\frac{\partial L}{\partial v} = \tau_t \tag{2.1}$$

$$\frac{d}{dt}\frac{\partial L}{\partial \omega} + \hat{\omega}\frac{\partial L}{\partial \omega} + \hat{v}\frac{\partial L}{\partial v} = \tau_r \ , \tag{2.2}$$

$$\frac{d}{dt}\frac{\partial L}{\partial \dot{\xi}} - \frac{\partial L}{\partial \xi} + \frac{\partial R}{\partial \dot{\xi}} = 0 \ , \tag{2.3}$$

where $\hat{a}$ denotes a 3×3 skew-symmetric matrix formed from $a = (a_1, a_2, a_3) \in \mathbf{R}^3$:

$$\hat{a} = \begin{bmatrix} 0 & -a_3 & a_2 \\ a_3 & 0 & -a_1 \\ -a_2 & a_1 & 0 \end{bmatrix}$$

Note that equations (2.1)-(2.2) are Kirchhoff's equations [23] for the base-body motion and equation (2.3) is Lagrange's equation for the internal motion. It must be pointed out that in the above formulation it is assumed that no control forces or torques exist that directly control the internal dynamics. The objective is to simultaneously control the rigid body dynamics and the internal dynamics using only control effectors that act on the rigid body; the control of internal dynamics must be achieved through the system coupling. In this regard, equations (2.1)-(2.3) model interesting examples of underactuated mechanical systems.

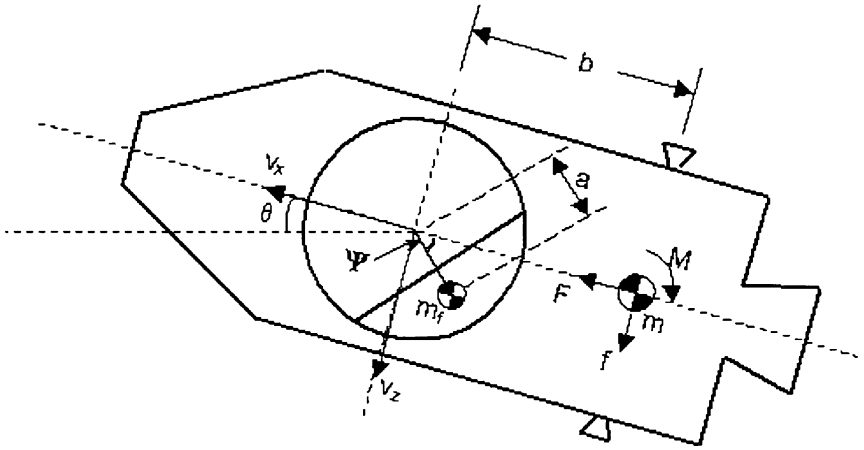

Figure 2.1: Single tank model.

The formulation using pendulum analogy can be summarized as follows. Consider a rigid spacecraft moving in a fixed plane as indicated in Figure 2.1. The state variables shown are the axial and transverse components of the velocity vector, v_x, v_z, the attitude angle θ of the spacecraft with respect to a fixed reference, and the angle ψ of the pendulum with respect to the spacecraft longitudinal axis, representing the fuel slosh. The engine exerts a thrust F along the longitudinal centerline and a torquer, such as a momentum wheel exerts a variable torque M about the spacecraft's center of mass. Side thrusters exert a lateral force, f, that acts through the base

body's center of mass. The constants in the problem are the spacecraft mass m and moment of inertia I (without fuel), the fuel mass m_f and moment of inertia I_f (assumed constant), the length $a > 0$ of the pendulum, and the distance b between the pendulum point of attachment and the spacecraft center of mass location along the longitudinal axis; if the pendulum point of attachment is in front of the spacecraft center of mass then $b > 0$. The parameters m_f, I_f and a depend on the shape of the fuel tank, the characteristics of the fuel and the fill ratio of the fuel tank.

Under the indicated assumptions, the kinetic energy of the base-body/pendulum system can be expressed as:

$$T = \frac{1}{2}m[v_x^2 + (v_z + b\dot{\theta})^2] + \frac{1}{2}I\dot{\theta}^2 + \frac{1}{2}I_f(\dot{\theta} + \dot{\psi})^2 + \frac{1}{2}m_f[(v_x + a(\dot{\theta} + \dot{\psi})\sin\psi)^2 + (v_z + a(\dot{\theta} + \dot{\psi})\cos\psi)^2] \ , \quad (2.4)$$

where the first term refers to the base-body translational kinetic energy, the second to the base-body rotational kinetic energy, the third to the fuel-mass rotational kinetic energy, and the final term expresses the fuel-mass translational kinetic energy.

Since gravitational effects are ignored, there is no potential energy. Thus, the Lagrangian equals the kinetic energy, i.e. $L = T$ Applying Kirchoff's equations with

$$R = \frac{1}{2}\epsilon\dot{\psi}^2. \ v = \begin{bmatrix} v_x \\ 0 \\ v_z \end{bmatrix}, \ \omega = \begin{bmatrix} 0 \\ \dot{\theta} \\ 0 \end{bmatrix}, \ \tau_t = \begin{bmatrix} F \\ 0 \\ f \end{bmatrix}, \ \tau_r = \begin{bmatrix} 0 \\ M + bf \\ 0 \end{bmatrix}, \quad (2.5)$$

where ϵ is the viscous damping constant, the equations of motion can be obtained as

$$(m + m_f)(\dot{v}_x + \dot{\theta}v_z) + m_f a(\ddot{\theta} + \ddot{\psi})\sin\psi + mb\dot{\theta}^2 + m_f a(\dot{\theta} + \dot{\psi})^2\cos\psi = F \ , \quad (2.6)$$

$$(m+m_f)(v_z-\theta v_x)+m_f a(\theta+\psi)\cos\psi+mb\theta-m_f a(\theta+\psi)^2\sin\psi=f\ , \qquad (2\ 7)$$

$$(I+mb^2)\theta+mb(v_z-\theta v_x)-\epsilon\psi=M+bf\ , \qquad (2\ 8)$$

$$(I_f+m_f a^2)(\theta+\psi)+m_f a(v_x+\theta v_z)\sin\psi+m_f a(v_z-\theta v_x)\cos\psi+\epsilon\psi=0 \qquad (2\ 9)$$

The control objective is to design feedback controllers so that the controlled spacecraft accomplishes a given planar maneuver, that is a change in the translational velocity vector and the attitude of the spacecraft, while attenuating the slosh mode

2.3 Second Order Systems

The spacecraft slosh problem, by its very nature, requires a solution that seeks to minimize the oscillatory motion of the propellant Any single-mode oscillatory system can be represented in differential form as [24]

$$\ddot{\psi}+2\zeta\omega\dot{\psi}+\omega^2\psi=\tau\ , \qquad (2\ 10)$$

where ψ is our generalized coordinate, ω is the undamped natural frequency of the system, τ is any externally applied force (or torque), and ζ is the damping ratio of the system Any $\zeta > 0$ implies the presence of damping (a certainty with any viscous fluid) If $\zeta > 1$, then the system is "overdamped" The "critically damped' case occurs when $\zeta = 1$ Either of these situations causes the system position ψ to approach the equilibrium point exponentially (as it would for an *extremely* viscous fluid) In a critically or overdamped system, the adverse effect on spacecraft attitude would be trivially manageable Therefore, in the slosh problem discussed here, the system is assumed to be "underdamped" (i e $0 < \zeta < 1$) This results in the detrimental oscillatory motion that demands design consideration

Chapters 3 and 4 will develop specific control laws to stabilize the system about equilibrium. Thus, the external torque τ in equation (2.10) will take a form proportional to those control inputs, u. In all of those developments, equation (2.10) will appear as:

$$\ddot{\psi} + 2\zeta\omega\dot{\psi} + \omega^2\psi = -\alpha u \ , \tag{2.11}$$

where α is the control proportionality constant. Taking the Laplace transform of equation (2.11) and rearranging, one finds the control-slosh angle transfer function:

$$\frac{\Psi}{U} = \frac{-\alpha}{s^2 + 2\zeta\omega s + \omega^2} \ . \tag{2.12}$$

where Ψ and U are the Laplace transforms of ψ and u, respectively. Equation (2.12) expresses the slosh dynamics of the system, and is considered in every linearization-based controller design scheme discussed in this thesis. It also illuminates the nature of the problem (and possible solutions): any linear controller that fails to lesson the impact of the denominator of the slosh transfer function in equation (2.12) risks exciting the system state.

2.4 Linearization

The controllers developed in Chapter 3 are linear, and thus require linearization of the equations of a motion about the equilibrium point. To obtain the linearized equations equations of motion, we first rewrite (2.6)-(2.9) as:

$$(m + m_f)a_x + m_f a(\ddot{\theta} + \ddot{\psi})\sin\psi + mb\dot{\theta}^2 + m_f a(\dot{\theta} + \dot{\psi})^2\cos\psi = F \ , \tag{2.13}$$

$$(m + m_f)a_z + m_f a(\ddot{\theta} + \ddot{\psi})\cos\psi + mb\ddot{\theta} - m_f a(\dot{\theta} + \dot{\psi})^2\sin\psi = f \ , \tag{2.14}$$

$$(I + mb^2)\theta + mba_z - \epsilon\psi = M + bf \ , \tag{2 15}$$

$$(I_f + m_f a^2)(\theta + \psi) + m_f a a_x \sin\psi + m_f a a_z \cos\psi + \epsilon\psi = 0 \ , \tag{2 16}$$

where $a_x = v_x + \theta v_z$ and $a_z = v_z - \theta v_x$ are the axial and transverse components of the acceleration vector The number of equations of motion can be reduced to two by solving equations (2 13) and (2 14) for a_x and a_z, and eliminating these accelerations from equations (2 15) and (2 16)

$$(I + mb^2)\theta - \frac{mb}{m + m_f}[m_f a(\theta + \psi)\cos\psi + mb\theta - m_f a(\theta + \psi)^2 \sin\psi - f] - \epsilon\psi = M + bf \ , \tag{2 17}$$

$$(I_f + m_f a^2)(\theta + \psi) + \frac{m_f a}{m + m_f}[F \sin\psi + f\cos\psi - m_f a(\theta + \psi) - mb\theta^2 \sin\psi - mb\theta\cos\psi] + \epsilon\psi = 0 \tag{2 18}$$

Without loss of generality, we will assume that the desired equilibrium for $M = 0$ and $f = 0$ is given by

$$\boldsymbol{x}^* = [\ \theta^* \quad \theta^* \quad \psi^* \quad \psi^*\ ]^T = [\ 0 \quad 0 \quad 0 \quad 0\ ]^T \tag{2 19}$$

When θ, ψ, and ψ are assumed to be small, equations (2 17)-(2 18) can be linearized around the desired equilibrium as

$$(I + mb^2)\theta - \frac{mb}{m + m_f}[m_f a(\theta + \psi) + mb\theta - f] - \epsilon\psi = M + bf \ , \tag{2 20}$$

$$(I_f + m_f a^2)(\ddot{\theta} + \ddot{\psi}) + \frac{m_f a}{m + m_f}[F\psi + f - m_f a(\ddot{\theta} + \ddot{\psi}) - mb\ddot{\theta}] + \epsilon\dot{\psi} = 0 \qquad (2.21)$$

The following simplifications are made:

$$m^* = \frac{mm_f}{m + m_f}, \quad I^* = I + m^*(b^2 - ab), \quad I_c^* = m^* ab, \quad I^{**} = I_f + m^*(a^2 - ab),$$
$$I_f^* = I_f + m^* a^2, \quad a^* = \frac{m_f a}{m + m_f}, \quad b^* = \frac{m_f b}{m + m_f} \qquad (2.22)$$

Substituting these into equations (2.20)-(2.21) and collecting terms, the final linearized equations of motion are obtained.

$$I^*\ddot{\theta} - I_c^*\ddot{\psi} - \epsilon\dot{\psi} = M + b^* f \ , \qquad (2.23)$$

$$I^{**}\ddot{\theta} + I_f^*\ddot{\psi} + \epsilon\dot{\psi} + a^* F\psi + a^* f = 0 \qquad (2.24)$$

2.4.1 Torquer Only

When setting $f = 0$, the linearized equations of motion become:

$$I^*\ddot{\theta} - I_c^*\ddot{\psi} - \epsilon\dot{\psi} = M \ , \qquad (2.25)$$

$$I^{**}\ddot{\theta} + I_f^*\ddot{\psi} + \epsilon\dot{\psi} + a^* F\psi = 0 \qquad (2.26)$$

By defining the pitch angular acceleration as the new control u, we can rewrite the linearized equations of motion as

$$\ddot{\theta} = u \ , \qquad (2.27)$$

$$\ddot{\psi} + 2\zeta_1\omega_1\dot{\psi} + \omega_1^2\psi = -\alpha_1 u \ , \qquad (2.28)$$

where

$$u = \frac{1}{I^* + \alpha_1 I_c^*}[M - I_c^* \omega_1^2 \psi + (\epsilon - 2\zeta_1 \omega_1 I_c^*)\dot{\psi}] \ , \tag{2.29}$$

$$\alpha_1 = \frac{I^{**}}{I_f^*} \ , \tag{2.30}$$

$$2\zeta_1 \omega_1 = \frac{\epsilon}{I_f^*} \ , \tag{2.31}$$

$$\omega_1^2 = \frac{a^* F}{I_f^*} \tag{2.32}$$

2.4.2 Side Thruster Only

When the torquer is turned off ($M = 0$) the linearized equations of motion become:

$$I^* \ddot{\theta} - I_c^* \ddot{\psi} - \epsilon \dot{\psi} = b^* f \ , \tag{2.33}$$

$$I^{**} \ddot{\theta} + I_f^* \ddot{\psi} + \epsilon \dot{\psi} + a^* F \psi = -a^* f \tag{2.34}$$

Again, the pitch angular acceleration is the control input, u. Rewriting the linearized equations of motion as

$$\ddot{\theta} = u \ , \tag{2.35}$$

$$\ddot{\psi} + 2\zeta_2 \omega_2 \dot{\psi} + \omega_2^2 \psi = -\alpha_2 u \ , \tag{2.36}$$

where

$$u = \frac{1}{I^* + \alpha_2 I_c^*}[b^* f - I_c^* \omega_2^2 \psi + (\epsilon - 2\zeta_2 \omega_2 I_c^*)\dot{\psi}] \ , \tag{2.37}$$

$$\alpha_2 = 1 + \frac{a}{b}\frac{I}{I_f} \ , \tag{2.38}$$

$$2\zeta_2 \omega_2 = (1 - \frac{a}{b})\frac{\epsilon}{I_f} \ , \tag{2.39}$$

$$\omega_2^2 = \frac{a^* F}{I_f} \tag{2.40}$$

For the oscillatory system of this thesis, ω is the undamped natural frequency of the slosh mode and ζ is the damping ratio of the system (see Section 2.3 on second-order systems). Any $\zeta > 0$ implies the presence of damping (a certainty with any viscous fluid).

Chapter 3 will develop specific control laws to stabilize the system about the equilibrium.

2.5 Controller Types

Regardless of the control law chosen, all controllers in this research have the same overall form. A "closed-loop" control system is shown in Figure 2.2. A desired

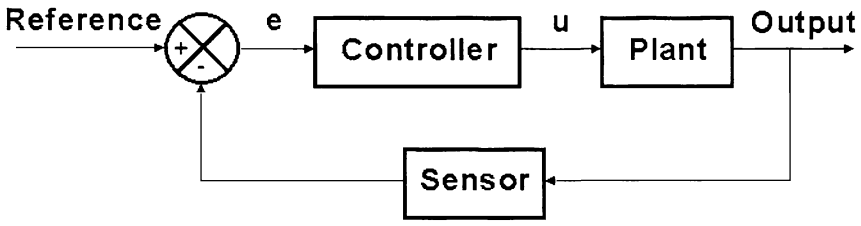

Figure 2.2: Block diagram of a closed-loop control system.

system state, or reference state is fed into the system-controller combination. The actual state, measured by a sensor device of some sort, is subtracted from the desired state. This difference is called the error, or e signal. The error is passed to the system controller, which may take many forms depending on the desired control action characteristics. The controller output u acts on the system plant, which is merely the mathematical model of the system one seeks to control. The resulting output is finally measured and subtracted from the reference to produce a new error signal. In any controlled system, it is desirable to minimize the difference between

the desired and actual system state; to drive the error signal to zero. In a closed-loop system, such as that shown above, the error signal is computed and acted upon every sampling time over the course of the system's operation. In an open-loop system the error signal is found (or guessed based on experience) only at the beginning of the time considered and the controller acts without the continuous feedback provided by the sensor branch shown. Thus, an open-loop system lacks the sensor feedback branch.

Common types of controllers include two-position (on-off), proportional, derivative, integral, or combinations of these. Two-position controllers, as the name implies, exclude the possibility of scalable input. Integral controllers are advantageous when a system is subject to noise-like disturbances not encountered in this research.

In the proportional controller, the control action is simply proportional to the error signal e. In the time-domain, this action would be represented by:

$$u(t) = K_p e(t) \tag{2.41}$$

Accordingly, the controller portion of the signal flow would be represented in block form as in Figure 2.3: The proportionality constant, K_p is adjustable to produce the

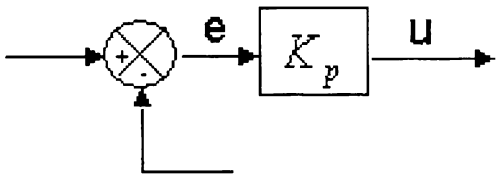

Figure 2.3: Proportional controller.

desired speed of response. For example; if the control action was that of a momentum wheel, a larger value of K_p would cause a greater wheel torque for a given error signal magnitude. Obviously, this simplest of controllers considers only the system state,

and not its rate of change. For this reason, the proportional controller may fail to adequately govern the system during periods of rapid change in state. Also, a simple proportional controller would drive the system past the desired state when the error signal approaches zero.

To solve this problem, the proportional-derivative (PD) controller is utilized.

$$u(t) = K_p e(t) + K_d \frac{de(t)}{dt} \tag{2.42}$$

Taking the Laplace transform of equation (2.42) is advantageous in that the differential form of the system may be expressed in algebraic form. The control signal's Laplace transform would be:

$$U(s) = K_p E(s) + K_d s E(s) \tag{2.43}$$

The controller portion of the signal flow would appear in block form as in Figure 2.4: It's easily seen that the PD controller is simply a linear combination of actions

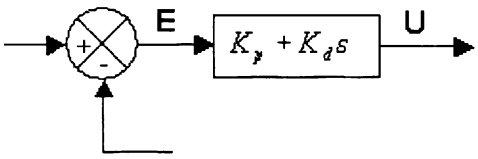

Figure 2.4: Proportional-derivative (PD) controller.

proportional to the error signal, and the time-derivative of the error signal. The proportional-derivative controller constants K_p and K_d are both adjusted to produce the desired response. In our momentum wheel example, if one chooses a large value for K_d, a higher torque will resist a sudden deviation from the desired state, even before the error signal has grown to a significant value. Thus, a PD controller can be thought to "anticipate" deviations from desired system behavior. This is the

commonly used controller chosen for one of the control algorithms in this thesis

Also, it should be noted that in the practical application of any controller combination, it may be necessary to adjust multiple proportionality constants, even those seemingly independent of each other, in order to produce the response times and reaction strengths the equipment can tolerate

2.6 State Space Representation

Consider the linearized equations

$$\theta = u \ , \tag{2 44}$$

$$\psi + 2\zeta\omega\psi + \omega^2\psi = -\alpha u \ , \tag{2 45}$$

where ζ, ω, and α for each actuator case are described by equations (2 30)-(2 32) and (2 38)-(2 40) For the linearized system (2 44)-(2 45) the state variables are the base body orientation angle θ, the slosh angle ψ, and their time derivatives The collection of these state variables is defined as the state vector, which is given by

$$\boldsymbol{x} = [\theta \ \ \dot{\theta} \ \ \psi \ \ \dot{\psi}]^T \tag{2 46}$$

Consequently, the state space equations can be written as

$$\dot{\boldsymbol{x}} = \boldsymbol{A}\boldsymbol{x} + \boldsymbol{B}\boldsymbol{u} \ , \tag{2 47}$$

where

$$\boldsymbol{A} = \begin{bmatrix} 0 & 1 & 0 & 0 \\ 0 & 0 & 0 & 0 \\ 0 & 0 & 0 & 1 \\ 0 & 0 & -\omega^2 & -2\zeta\omega \end{bmatrix}, \quad \boldsymbol{B} = \begin{bmatrix} 0 \\ 1 \\ 0 \\ -\alpha \end{bmatrix} \tag{2.48}$$

The system (2.47) is Linear Time-Invariant (LTI), and will form the basis of the design of linear controllers. As will be shown later, some auxiliary quantities such as filter state variables may be added to the state vector to serve as intermediary tools in the formulation of the linear controllers.

2.7 Controllability

For an LTI system given in the form of equation (2.47), it is advisable to determine whether the system is controllable before beginning the controller design process. This is accomplished by considering the *controllability matrix* of the system.

$$\boldsymbol{Co} = [\ \boldsymbol{B}\ |\ \boldsymbol{AB}\ |\ \cdot\cdot\ |\ \boldsymbol{A}^{n-1}\boldsymbol{B}\ ], \tag{2.49}$$

where $\boldsymbol{A}$ is the system's state matrix, and $\boldsymbol{B}$ is the input matrix discussed previously. If the $rank(\boldsymbol{Co}) = n$, then the system is completely state controllable.

Consider the linearized system (2.47). Clearly, $n = 4$ and

$$\boldsymbol{Co} = [\ \boldsymbol{B}\ |\ \boldsymbol{AB}\ |\ \boldsymbol{A^2B}\ |\ \boldsymbol{A^3B}\ ]$$
$$= \begin{bmatrix} 0 & 1 & 0 & 0 \\ 1 & 0 & 0 & 0 \\ 0 & -\alpha & 2\alpha\zeta\omega & \alpha\omega^2(1-4\zeta^2) \\ -\alpha & 2\alpha\zeta\omega & \alpha\omega^2(1-4\zeta^2) & -4\alpha\zeta\omega^3(1-2\zeta^2) \end{bmatrix} \tag{2.50}$$

Since $rank(\boldsymbol{Co}) = 4$, the linearized system is completely controllable. This means that one can design feedback controllers to arbitrarily assign the eigenvalues of the closed-loop system.

Chapter 3 will call upon the transfer function and state-space representations of the pendulum fuel slosh model in the design of linearized controllers.

Chapter 3

Linearization Based Controller Design

3.1 Introduction

In this chapter we use the model presented in Section 2.2 to develop linear controllers designed to control the slosh and transverse dynamics of the spacecraft during a maneuver. As discussed in Section 2.4; θ, $\dot{\theta}$, ψ, and $\dot{\psi}$ are assumed to be small, resulting in the second order form represented by equation (2.24). First, a proportional-plus-derivative (PD) slosh controller is developed utilizing only the spacecraft torquer, and then only the side-thrusters. It will be demonstrated that, in both cases, undesirable steady-state offsets in lateral velocity occur. The same offsets are present for the torquer only, thruster only cases developed utilizing a linear quadratic regulator (LQR) synthesis. These results are consistent with those seen in Wie [11]. Finally, for each controller, a two-phase (or switched) controller is utilized that stabilizes first the rigid-body attitude and slosh dynamics via the torquer, and then the lateral velocity via the side-thrusters.

3.2 PD Controller with Generalized Filter

As shown in the previous chapter, the linearized equations can be written as

$$\ddot{\theta} = u \,, \tag{3.1}$$

$$\ddot{\psi} + 2\zeta\omega\dot{\psi} + \omega^2\psi = -\alpha u \tag{3.2}$$

It is desirable to apply control inputs affecting the spacecraft orientation without exciting the slosh mode. The second order system behavior of the fuel mass can be represented by the transfer function:

$$\frac{\Psi}{U} = \frac{-\alpha}{s^2 + 2\zeta\omega s + \omega^2} \tag{3.3}$$

With this behavior known, it is possible to design a control system possessing a range of inputs that prevents excitation by attenuating control signals that will excite the slosh mode. The block diagram form of the complete control system is shown in Figure 3.1. In the figure, θ_c is the desired rigid-body orientation angle, u_f is the basic PD

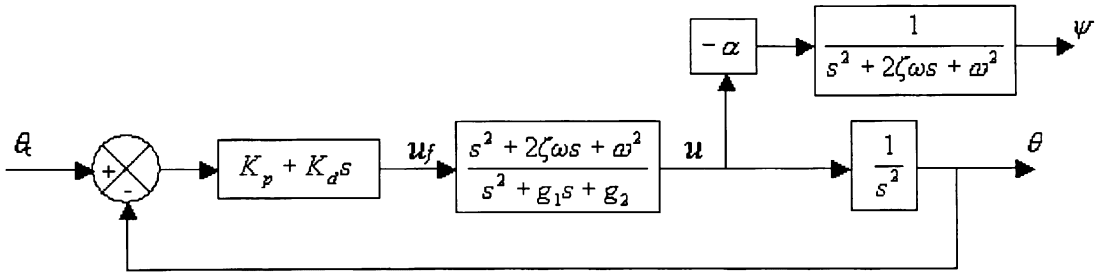

Figure 3.1: PD controller with generalized filter.

control signal, g_1 and g_2 are the generalized filter coefficients, u is the actual applied control signal, and θ and ψ are the resulting spacecraft and fuel mass orientation angles, respectively. It is evident when considering the slosh-angle transfer function

that the numerator of the generalized filter and denominator of the slosh dynamics blocks will cancel, thus eliminating the adverse effects control inputs.

The output of the PD controller (with $\theta_c = 0$) is given by

$$u_f = -K_p\theta - K_d\dot{\theta} \,, \tag{3.4}$$

where K_p and K_d represent the controller gains.

The generalized filter can be expressed as a transfer function from the input u_f to the filter output u as:

$$\frac{u}{u_f} = \frac{s^2 + 2\zeta\omega s + \omega^2}{s^2 + g_1 s + g_2} \,, \tag{3.5}$$

or, equivalently, in differential equation form as:

$$\ddot{u} + g_1\dot{u} + g_2 u = \ddot{u}_f + 2\zeta\omega\dot{u}_f + \omega^2 u_f \tag{3.6}$$

To obtain a state-space realization of the filter, define an auxiliary signal z such that:

$$\ddot{z} + g_1\dot{z} + g_2 z = u_f \,, \tag{3.7}$$

so that the transfer function from u_f to z becomes:

$$\frac{z}{u_f} = \frac{1}{s^2 + g_1 s + g_2} \tag{3.8}$$

Dividing equation (3.5) by (3.8) yields:

$$\frac{u}{z} = s^2 + 2\zeta\omega s + \omega^2 \,, \tag{3.9}$$

which can be equivalently written in differential equation form as

$$u = z + 2\zeta\omega z + \omega^2 z \tag{3 10}$$

Substituting z from equation (3 7) and u_f from equation (3 4) the control law can be written as

$$u = -K_p\theta - K_d\theta + (2\zeta\omega - g_1)z + (\omega^2 - g_2)z \tag{3 11}$$

3.2.1 Torquer Only

First, control of the spacecraft attitude and slosh dynamics is attempted with only the onboard torquer (a reaction wheel, a control moment gyro, or a pair of gas jet thrusters) Equation (2 18) is used, setting $f = 0$ Collecting terms and using the substitutions specified in equation (2 22), the nonlinear slosh dynamics can be expressed as

$$\psi = \left[\frac{I_c^*}{I_f^*}\cos\psi - 1\right]\theta + \frac{I_c^*}{I_f^*}\theta^2 \sin\psi - \frac{\epsilon}{I_f^*}\psi - \frac{a^*}{I_f^*}F\sin\psi \tag{3 12}$$

Note that the linearized equations for this case are given by (3 1)-(3 2) with $\alpha = \alpha_1$, $\omega = \omega_1$, $\zeta = \zeta_1$ as described in Section 2 4 1

Define the state variables

$$(x_1,\ x_2,\ x_3,\ x_4,\ x_5,\ x_6) = (\theta,\ \theta,\ \psi\ \ \psi,\ z,\ z)\ ,$$

so that the state equations can be written as

$$x_1 = x_2 \tag{3 13}$$

$$\dot{x}_2 = u \ , \tag{3.14}$$

$$\dot{x}_3 = x_4 \ . \tag{3.15}$$

$$\dot{x}_4 = b_1(x)u + c_1(x) \ , \tag{3.16}$$

$$\dot{x}_5 = x_6 \ , \tag{3.17}$$

$$\dot{x}_6 = -K_p x_1 - K_d x_2 - g_2 x_5 - g_1 x_6 \ , \tag{3.18}$$

where

$$u = -K_p x_1 - K_d x_2 + (\omega_1^2 - g_2)x_5 + (2\zeta_1\omega_1 - g_1)x_6 \ , \tag{3.19}$$

and

$$b_1(x) = \left[\frac{I_c^*}{I_f^*} \cos x_3 - 1 \right] \ ,$$

$$c_1(x) = \frac{I_c^*}{I_f^*} x_2^2 \sin x_3 - \frac{\epsilon}{I_f^*} x_4 - \frac{a^*}{I_f^*} F \sin x_3$$

Having chosen values for the physical parameters of the system and the values of control parameters K_p, K_d, g_1, and g_2; one can numerically integrate equations (3.13)-(3.18) for any initial conditions. The resulting control inputs are applied to the original nonlinear equations of motion (equations (2.6)-(2.9)) to evaluate controller performance. The results are shown in Figures 5.1 and 5.2. The first illustrates the state values θ, ψ, v_x, and v_z throughout the maneuver. The equations of motion (2.7) and (2.8) are solved for the actuator inputs M and f to produce the second figure ($f = 0$ at all times in this case). It is expected that a linear controller (such as this one) will produce undesirable slosh and transverse responses during aggressive maneuvers.

3.2.2 Side-Thrusters Only

As with the torquer, we seek to explore attitude performance with only the side thrusters. Again, the equations of motion are reduced to two by eliminating the a_x and a_z acceleration terms. Setting the torquer input, $M = 0$, collecting terms, and using equation (2.22), the nonlinear slosh dynamics are:

$$\begin{aligned}\ddot{\psi} = &-\frac{\left(I_f^* + \frac{a}{b} I \cos\psi - m^* a^2 \cos^2\psi\right)}{I_f^* - m^* a^2 \cos^2\psi}\ddot{\theta} - \frac{\left(1 - \frac{a}{b}\cos\psi\right)\epsilon\dot{\psi}}{I_f^* - m^* a^2 \cos^2\psi} \\ &+ \frac{I_c^* \dot{\theta}^2 \sin\psi}{I_f^* - m^* a^2 \cos^2\psi} - \frac{a^* F \sin\psi}{I_f^* - m^* a^2 \cos^2\psi} - \frac{m^* a^2 \dot{\theta}^2 \sin\psi\cos\psi}{I_f^* - m^* a^2 \cos^2\psi} \\ &- \frac{2m^* a^2 \dot{\theta}\dot{\psi} \sin\psi\cos\psi}{I_f^* - m^* a^2 \cos^2\psi} - \frac{m^* a^2 \dot{\psi}^2 \sin\psi\cos\psi}{I_f^* - m^* a^2 \cos^2\psi} \end{aligned} \tag{3.20}$$

Note that the linearized equations for this case are given by (3.1)-(3.2) with $\alpha = \alpha_2$, $\omega = \omega_2$, $\zeta = \zeta_2$ as described in Section 2.4.1.

Again define the state variables

$$(x_1,\ x_2,\ x_3,\ x_4,\ x_5,\ x_6) = (\theta,\ \dot{\theta},\ \psi,\ \dot{\psi},\ z,\ \dot{z})\ ,$$

so that the state equations can be written as:

$$\dot{x}_1 = x_2\ , \tag{3.21}$$

$$\dot{x}_2 = u\ , \tag{3.22}$$

$$\dot{x}_3 = x_4\ , \tag{3.23}$$

$$\dot{x}_4 = b_2(x)u + c_2(x)\ , \tag{3.24}$$

$$\dot{x}_5 = x_6\ . \tag{3.25}$$

$$x_6 = -K_p x_1 - K_d x_2 - g_2 x_5 - g_1 x_6 \ , \tag{3 26}$$

where

$$u = -K_p x_1 - K_d x_2 + (\omega_2^2 - g_2) x_5 + (2\zeta_2 \omega_2 - g_1) x_6 \ , \tag{3 27}$$

and

$$b_2(x) = -\frac{\left(I_f^* + \frac{a}{b} I \cos x_3 - m^* a^2 \cos^2 x_3\right)}{I_f^* - m^* a^2 \cos^2 x_3} \ ,$$

$$c_2(x) = -\frac{\left(1 - \frac{a}{b}\cos x_3\right) \epsilon x_4}{I_f^* - m^* a^2 \cos^2 x_3} + \frac{I_c^* x_2^2 \sin x_3}{I_f^* - m^* a^2 \cos^2 x_3} - \frac{a^* F \sin x_3}{I_f^* - m^* a^2 \cos^2 x_3} - \frac{m^* a^2 x_2^2 \sin x_3 \cos x_3}{I_f^* - m^* a^2 \cos^2 x_3}$$

$$- \frac{2m^* a^2 x_2 x_4 \sin x_3 \cos x_3}{I_f^* - m^* a^2 \cos^2 x_3} - \frac{m^* a^2 x_4^2 \sin x_3 \cos x_3}{I_f^* - m^* a^2 \cos^2 x_3}$$

Again having chosen values for the physical parameters of the system and the values of control parameters K_p, K_d, g_1, and g_2, one can numerically integrate equations (3 21)-(3 26) for any initial conditions As before, the resulting control inputs are applied to the original nonlinear equations of motion (equations (2 6)-(2 9)) to evaluate controller performance Figures 5 3 and 5 4 demonstrate these results

3.2.3 2-Phase Feedback

The results of sections 3 2 1 and 3 2 2 reveal the inability of a spacecraft with a single actuator to drive the pitch and slosh angles to zero without enhancing the transverse velocity In this section, a two-phase or "switched" feedback controller is developed that drives the pitch and slosh angle to zero using the onboard torquer, and then, while maintaining this rigid-body attitude, stabilizes the lateral velocity with thruster input Generalized filters similar to that developed in Section 3 2 accomplish each of these tasks

First, define u_1 to be pitch acceleration and u_2 to be the lateral acceleration In the first phase of the maneuver the closed-loop equations of motion are identical to those

of the torquer-only case found in Section 3.2.1. When the norm of the partial state vector $\|\boldsymbol{x}\| = \sqrt{\theta^2 + \dot{\theta}^2 + \psi^2 + \dot{\psi}^2}$ falls below a specified error condition (10^{-6}, for example), the controller switches to the second phase. In this phase, the rigid-body attitude angle is kept at zero by setting the pitch control law to:

$$u_1 = -2\lambda\dot{\theta} - \lambda^2\theta \,, \tag{3.28}$$

where λ is a positive gain value. For a spacecraft whose pitch and slosh angle has already been driven nearly to zero, the form of equation (3.28) ensures that the angle will continue to be driven to zero by virtue of its negative eigenvalues. Thus, the momentum wheel acts to maintain the acheived rigid-body orientation while the thruster forces drive the lateral velocity accumulated in phase one to zero. Therefore, the closed-loop equations of motion are identical to equations (3.13)-(3.18), with the exceptions of the substitution of pitch control law equation (3.28) for equation (3.14), and the substitution of slosh dynamics equation (3.29) found by including both M and f in a solution of equations (2.6)-(2.9):

$$\begin{aligned}\ddot{\psi} = &-\frac{\epsilon}{I_f + m^*a^2 + a^*m_f a\cos^2\psi}\dot{\psi} - u_1 \\ &- \frac{m_f a\cos\psi}{I_f + m^*a^2 + a^*m_f a\cos^2\psi}u_2 - \frac{a^*F\sin\psi}{I_f + m^*a^2 + a^*m_f a\cos^2\psi} \\ &+ \frac{I_c^*\dot{\theta}^2\sin\psi}{I_f + m^*a^2 + a^*m_f a\cos^2\psi} + \frac{a^*m_f a(\dot{\theta}^2 + \dot{\psi}^2)\sin\psi\cos\psi}{I_f + m^*a^2 + a^*m_f a\cos^2\psi}\end{aligned} \tag{3.29}$$

Equation (3.29) includes the lateral acceleration controller u_2. This controller is a generalized filter with coefficients h_1 and h_2. The PD output seen in the pitch-angle controller is not used for the velocity control. Instead, a simpler *proportional* controller acts on v_z. Therefore, the auxiliary equation (3.18), and subsequent u_2

control become

$$x_6 = z = -K_{vz}v_z - h_1 z - h_2 z \ , \tag{3 30}$$

$$u_2 = -K_{vz}v_z + (2\zeta_{vz}\omega_{vz} - h_1)z + (\omega_{vz}^2 - h_2)z \ , \tag{3 31}$$

where K_{vz} is the proportional gain, and ζ_{vz} and ω_{vz} are the damping coefficient and natural frequency of the second order system found when the system is linearized for the velocity controller assuming ψ, ψ, θ, θ, *and* θ are small in the second phase of the manuever Doing so, it can be shown that

$$\omega_{vz} = \sqrt{\frac{a^* F}{I_f + m_f a^2}} \ , \qquad \zeta_{vz} = \frac{\epsilon}{2\omega_{vz}(I_f + m_f a^2)} \ , \qquad \alpha_{vz} = \frac{m_f a}{I_f + m_f a^2} \tag{3 32}$$

(The velocity control proportionality constant, α_{vz}, will be used later) It's noted here that the auxiliary variables z and z used to compute the velocity control are not the same as those used in the pitch control, and are defined separately in the simulation coding Figures 5 5 and 5 6 show that this linear, switched controller does succeed in stabilizing the entire system, including the transverse velocity

3.3 LQR Control

A Linear Quadratic Regulator (LQR) controller drives the linear time-invariant system defined by equation (2 47) to the origin using the minimum cost as specified by a function of the control input u, and system state $\boldsymbol{x}$ The LQR controller is basically a linear feedback control law

$$u = -\boldsymbol{K}\boldsymbol{x} \tag{3 33}$$

that minimizes the quadratic cost function,

$$J = \int_0^\infty (\boldsymbol{x}^T \boldsymbol{Q} \boldsymbol{x} + \boldsymbol{u}^T \boldsymbol{R} \boldsymbol{u}) dt \ , \tag{3.34}$$

where $\boldsymbol{Q}$ is a symmetric positive-semidefinite weighting matrix and $\boldsymbol{R}$ is a symmetric positive-definite weighting matrix [25]. In our single input system, $\boldsymbol{R}$ will be simply a scalar. The diagonal elements of $\boldsymbol{Q}$ and magnitude of $\boldsymbol{R}$ can be chosen to affect the relative effort the control law assigns to driving particular state variables. For example, in our case, if it was deemed necessary to heavily suppress the slosh motion, the diagonal elements of $\boldsymbol{Q}$ corresponding to ψ and $\dot{\psi}$ would be orders of magnitude greater than those corresponding to θ and $\dot{\theta}$.

The optimal control gain matrix $\boldsymbol{K} = [k_1 \ k_2 \ k_3 \ k_4]$ is found by solving the matrix-Riccati equation. The optimum control law now known, the state equations for our second-order system becomes:

$$\dot{x}_1 = x_2 \tag{3.35}$$

$$\dot{x}_2 = -k_1 x_1 - k_2 x_2 - k_3 x_3 - k_4 x_4 \tag{3.36}$$

$$\dot{x}_3 = x_4 \tag{3.37}$$

$$\dot{x}_4 = \ddot{\psi} \tag{3.38}$$

The weighting matrices $\boldsymbol{Q}$ and $\boldsymbol{R}$ are created with the proper state variable suppression characterists in mind, as discussed above. The gain vector $\boldsymbol{K}$ can then quickly be found using any control-theory algorithm capable of solving the matrix-Riccati equation (such as MATLAB's *lqr* function). The form of equation (3.38) will depend on the actuator being used to control the system, and will be included in the following sections.

3.3.1 Torquer Only

As with the generalized filter, control is first sought with only the onboard torquer. Setting $f = 0$ in the LTI system of equations (2.23) and (2.24), the slosh dynamics can be expressed as:

$$\ddot{\psi} = -\omega^2\psi - 2\zeta\omega\dot{\psi} - \alpha u_1 \tag{3.39}$$

Using this approximation, the state-space matrices of equation (2.47) become:

$$\boldsymbol{A} = \begin{bmatrix} 0 & 1 & 0 & 0 \\ 0 & 0 & 0 & 0 \\ 0 & 0 & 0 & 1 \\ 0 & 0 & -\omega^2 & -2\zeta\omega \end{bmatrix}, \quad \boldsymbol{B} = \begin{bmatrix} 0 \\ 1 \\ 0 \\ -\alpha \end{bmatrix} \tag{3.40}$$

After choosing the spacecraft's physical parameters and the regulator's $\boldsymbol{Q}$ and $\boldsymbol{R}$ weighting matrices, the Riccati solver is invoked to produce the controller gain vector $\boldsymbol{K}$. This controller is then applied to the actual nonlinear system whose slosh mechanics, $\ddot{\psi}$, are identical to that found in equation (3.12); this relation is substituted into equation (3.38). Equations (3.35)-(3.38), as well as the $\dot{v}_x$ and $\dot{v}_z$ expressions, are integrated to simulate the system response. Figures 5.7 and 5.8 reveal the system response using the chosen physical parameters, $\boldsymbol{Q}$ and $\boldsymbol{R}$ gains, and initial conditions.

3.3.2 Side-Thrusters Only

Considering only the thrusters ($M = 0$), the slosh dynamics, $\ddot{\psi}$, are identical to the corresponding generalized filter case. With the LQR control law found in equation (3.33) and the slosh dynamics of equation (3.20), the complete system of equations are again integrated to simulate the response (Figures 5.9 and 5.10).

3.3.3 2-Phase Feedback

As with the generalized filter case, the performance of the controllers developed in Sections 3.3.1 and 3.3.2 show that an LQR controlled spacecraft with a single actuator fails to stabilize the transverse velocity during a pitch maneuver. Again, a two-phase controller is constructed to produce acceptable results. Just as with the generalized filter, the pitch and slosh dynamics are stabilized first using the rigid-body torquer. When the vehicle state vector has reached the chosen error threshold, the controller "switches" to transverse controller mode. The Linear Quadratic Regulator approach is used for both phases.

The first phase of the manuever utilizes a LQR controller identical to that developed in the torquer-only scenario (Section 3.3.1). Once the first-phase controller drives the attitude and slosh angle to nearly zero, the pitch controller u_1 becomes that shown in equation (3.28). The lateral acceleration controller, u_2, is a LQR controller acting on ψ, $\dot{\psi}$, and v_z. Using the same linearized system equations developed for the two-phase filter of Section 3.2.3, a regulator can be designed with the following state matrices:

$$\boldsymbol{A} = \begin{bmatrix} 0 & 1 & 0 \\ -\omega_{vz}^2 & -2\zeta_{vz}\omega_{vz} & 0 \\ 0 & 0 & 0 \end{bmatrix}, \quad \boldsymbol{B} = \begin{bmatrix} 0 \\ -\alpha_{vz} \\ 1 \end{bmatrix} \tag{3.41}$$

Having chosen (different) $\boldsymbol{Q}$ and $\boldsymbol{R}$ weighting matrices, the Riccati solver obtains the gain vector $\boldsymbol{K}_{vz}$ for the velocity controller. The slosh dynamics are then replaced by equation (3.29) which, again, includes u_2. The complete set of nonlinear equations of motion are integrated. Similar to the generalized filter case, a two-phase LQR controller does succeed in stabilizing the transverse spacecraft dynamics, as well as the pitch and slosh dynamics (see Figures 5.11 and 5.12).

Although the two-phase linear controllers succeed in driving the system to the de-

sired state, it is preferrable that a controller can be found that acts on the pitch, slosh, and transverse velocity dynamics simultaneously. For this, a nonlinear controller is required. Chapter 4 invokes Lyapunov's Second Method to stabilize the spacecraft in this manner.

Chapter 4

Lyapunov Based Nonlinear Controller Design

4.1 Background on Lyapunov Stability Theory

In any given system if the state diverges from the chosen equilibrium point, the controller has obviously failed to perform. Therefore, it is the goal to choose a controller that makes the chosen equilibrium state stable. Historically, the most common method to go about determining the stability of an equilibrium is to solve the differential equations of motion. Unfortunately, this may be impossible (or very difficult) for a nonlinear system. Aleksandr Lyapunov provided two means to approach the problem; his indirect and later, his direct method. The indirect method involves linearizing the system dynamics about the equilibrium and analyzing the eigenvalues of the linearized system. Lyapunov's direct method requires no linearization, and this is the approach that is explored in this chapter.

In order to briefly describe Lyapunov's direct, or second method, we first summarize concepts involved in Lyapunov's stability theory. For full detail, the reader is

referred to [26].

Let $\boldsymbol{x} = [x_1\ x_2 \cdots x_n]^T$ denote an n dimensional state vector and consider a nonlinear dynamical system written in the form

$$\dot{\boldsymbol{x}} = \boldsymbol{f}(\boldsymbol{x}, t)\ , \tag{4.1}$$

where the vector function $\boldsymbol{f}(\boldsymbol{x}, t)$ is considered to be continuous with respect to t. A vector $\boldsymbol{x}^*$ is said to be an equilibrium state of equation (4.1) if

$$\boldsymbol{f}(\boldsymbol{x}^*, t) = 0\ \ \forall t \geq 0$$

- The equilibrium state $\boldsymbol{x}^*$ is said to be *Lyapunov stable* if for all $t_0 \geq 0$ and $\epsilon > 0$, there exists a real positive number $\delta(\epsilon, t_0)$ such that

$$\|\boldsymbol{x}(t_0) - \boldsymbol{x}^*\| < \delta(\epsilon, t_0) \Rightarrow \|\boldsymbol{x}(t) - \boldsymbol{x}^*\| < \epsilon\ \ \forall t \geq t_0\ ,$$

  where $\|\boldsymbol{x}\| = \sqrt{\boldsymbol{x}^T\boldsymbol{x}}$.

- The equilibrium state $\boldsymbol{x}^*$ is said to be *locally asymptotically stable* if it is *Lyapunov stable* as explained above and if for all $t_0 \geq 0$ there exists a postive $\delta(t_0)$ such that

$$\|\boldsymbol{x}(t_0) - \boldsymbol{x}^*\| < \delta(t_0) \Rightarrow \lim_{t\to\infty} \|\boldsymbol{x}(t)\| = \boldsymbol{x}^*$$

- The equilibrium state $\boldsymbol{x}^*$ is said to be *globally asymptotically stable* if both of the above conditions are met for all initial conditions

Proving stability of nonlinear systems with the basic stability definitions and without resorting to local approximations can be quite tedious and difficult. Lyapunov's direct method provides a tool to make rigorous, analytical stability claims of nonlinear

systems by studying the behavior of a scalar, energy-like Lyapunov function

Let $V(\boldsymbol{x})$ be a continuously differentiable function defined on a domain $\mathbf{D}$, which contains the equilibrium state Then we have the following definitions

- $V(\boldsymbol{x})$ is said to be positive definite if $V(\boldsymbol{x}^*) = 0$ and

$$V(\boldsymbol{x}) > 0 \ \ \forall \boldsymbol{x} \in \mathbf{D} - \{\boldsymbol{x}^*\}$$

- $V(\boldsymbol{x})$ is positive semidefinite in the same domain if

$$V(\boldsymbol{x}) \geq 0 \ \ \forall \boldsymbol{x} \in \mathbf{D}$$

Negative definite and negative semidefinite are defined as if $-V(\boldsymbol{x})$ is positive definite and if $-V(\boldsymbol{x})$ is positive semidefinite, respectively

We now summarize Lyapunov's second stability theorem Consider the dynamical system (4 1) and assume that $\boldsymbol{x}^*$ is an isolated equilibrium state If a positive-definite scalar function $V(\boldsymbol{x})$ exists in the region $\mathbf{D}$ around the equilibrium state $\boldsymbol{x}^*$, with continuous first partial derivatives, where the following conditions are met

1) $V(\boldsymbol{x}) > 0$ for all $\boldsymbol{x} \neq \boldsymbol{x}^*$ in $\mathbf{D}$ and $V(\boldsymbol{x}^*) = 0$

2) $V(\boldsymbol{x}) \leq 0$ for all $\boldsymbol{x} \neq \boldsymbol{x}^*$ in $\mathbf{D}$

then the equilibrium point $\boldsymbol{x}^*$ is stable

If, in addition to 1 and 2,

3) $V(\boldsymbol{x})$ is not identically zero along any solution of the system (4 1) other than $\boldsymbol{x}^*$, then the equilibrium point $\boldsymbol{x}^*$ is locally asymptotically stable

If, in addition to 3,

4) there exists in the entire state space a positive-definite function $V(\boldsymbol{x})$ which is radially unbounded, i e , $V(\boldsymbol{x}) \to \infty$ as $\|\boldsymbol{x}\| \to \infty$, then the equilibrium point $\boldsymbol{x}^*$

is globally asymptotically stable.

Note that conditions 3 and 4 follow directly from LaSalle's principle. For a globally asymptotically stable system, the contour plot of the Lyapunov function $V(\boldsymbol{x})$ would resemble a bowl (Figure 4.1), where x_1 and x_2 are coordinates of any system, although

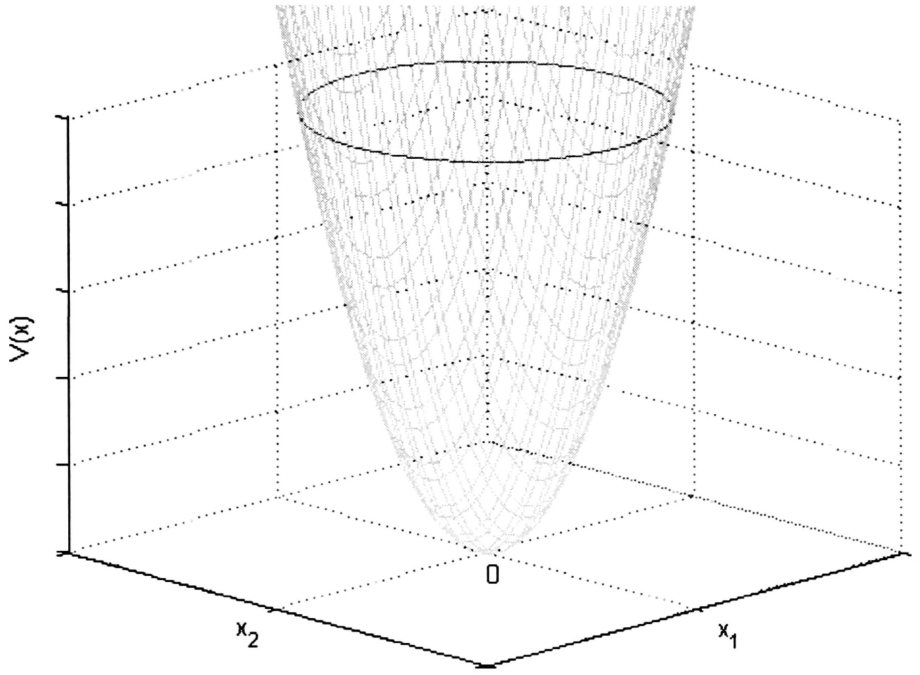

Figure 4.1: Energy-like Lyapunov function

the process can be generalized to higher dimensions. If the Lyapunov stability criteria are satisfied, then a system starting at any point on the surface defined by $V(\boldsymbol{x})$ will eventually converge to the origin $x_1^* = x_2^* = 0$.

4.2 Lyapunov-Based Controller

Following the previous work in [27], we consider a constant thrust $F > 0$ and design a Lyapunov-based feedback law to stabilize the system to a relative equilibrium defined by a constant acceleration in the axial direction.

Consider the system (2 6)-(2 9) If the axial thrust F is a positive constant and if the transverse force and pitching moment are zero, $f = M = 0$, then the spacecraft and fuel slosh dynamics have a relative equilibrium defined by

$$v_x^*(t) = \frac{F}{m + m_f} t + v_{x0} \ , \ v_z = v_z^* \ ,$$

$$\theta = \theta^* , \ \theta = 0 \ , \ \psi = 0 \ , \ \psi = 0 \, ,$$

where v_z^* and θ^* are arbitrary constants, and v_{x0} is the initial axial velocity of the spacecraft

Note that θ^* and v_z^* are desired system positions, chosen as zero in this research Now assume the axial acceleration term a_x is not significantly affected by pitch changes and fuel motion (an assumption verified in simulations) Consequently, equation (2 6) becomes

$$v_x + \theta v_z = \frac{F}{m + m_f} \tag{4 2}$$

The equations of motion can now be expressed as

$$(m + m_f)(v_z - \theta v_x(t)) + m_f a(\theta + \psi) \cos\psi + mb\theta - m_f a(\theta + \psi)^2 \sin\psi = f \ , \tag{4 3}$$

$$(I + mb^2)\theta + mb(v_z - \theta v_x(t)) - \epsilon\psi = M + bf \ , \tag{4 4}$$

$$(I_f + m_f a^2)(\theta + \psi) + m_f a \frac{F}{m + m_f} \sin\psi + m_f a(v_z - \theta v_x(t)) \cos\psi + \epsilon\psi = 0 \tag{4 5}$$

The axial velocity error variable takes the form

$$\tilde{v}_x = v_x(t) - v_x^*(t) \tag{4 6}$$

If, as in [28], the following intermediate control inputs are defined

$$\begin{bmatrix} u_1 \\ u_2 \end{bmatrix} = \boldsymbol{M}(\psi)^{-1} \begin{bmatrix} F - m_f a \psi \cos\psi + m_f a(\theta+\psi)^2 \sin\psi \\ M + Fb \end{bmatrix}, \tag{4 7}$$

where

$$\boldsymbol{M}(\psi) = \begin{bmatrix} m_f a \cos\psi + mb & m + m_f \\ I + mb^2 & mb \end{bmatrix}, \tag{4 8}$$

and

$$c = \frac{m_f a}{I_f + m_f a^2}\ , \quad d = \frac{Fc}{m + m_f}\ , \quad e = \frac{\epsilon}{I_f + m_f a^2}\ , \tag{4 9}$$

then the equations of motion can be further simplified to

$$\theta = u_1\ , \tag{4 10}$$

$$\psi = -u_2 c \cos\psi - u_1 - d \sin\psi - e\psi \tag{4 11}$$

$$\tilde{v}_x = -\theta v_z\ , \tag{4 12}$$

$$v_z = u_2 + \theta(\tilde{v}_x + v_x^*(t))\ , \tag{4 13}$$

As in [27], the candidate Lyapunov function chosen is

$$V = \frac{r_1}{2}(\tilde{v}_x^2 + v_z^2) + \frac{r_2}{2}\theta^2 + \frac{r_3}{2}\theta^2 + r_4 d(1 - \cos\psi) + \frac{r_4}{2}(\theta+\psi)^2\ , \tag{4 14}$$

where r_1, r_2, r_3, and r_4 are controller parameters The Lyapunov function V is positive definite if $r_i > 0$

Taking the time derivative of the above Lyapunov function along the trajectories

of equations (4.10)-(4.13) yields

$$\dot{V} = [r_1 v_z - r_4 c(\dot{\theta} + \dot{\psi}) \cos\psi] u_2 - r_4 e(\dot{\theta} + \dot{\psi})^2 + [r_1 v_x^*(t) v_z + r_2 \theta + r_3 u_1 + r_4 e(\dot{\theta} + \dot{\psi}) - r_4 d \sin\psi]\dot{\theta} \quad (4.15)$$

If the following final control laws are proposed:

$$u_1 = -l_2 \dot{\theta} - \left[\frac{r_1}{r_3} v_x^*(t) v_z + \frac{r_2}{r_3}\theta\right] - \frac{r_4}{r_3}[e(\dot{\theta} + \dot{\psi}) - d\sin\psi] \,, \quad (4.16)$$

$$u_2 = -l_1[r_1 v_z - r_4 c(\dot{\theta} + \dot{\psi})\cos\psi] \,, \quad (4.17)$$

where l_1 and l_2 are positive gains, $\dot{V}$ becomes:

$$\dot{V} = -l_1[r_1 v_z - r_4 c(\dot{\theta} + \dot{\psi})\cos\psi]^2 - l_2\dot{\theta}^2 - r_4 e(\dot{\theta} + \dot{\psi})^2 \quad (4.18)$$

It is clear that $\dot{V}$ is negative semidefinite and, thus, the system is stable about the desired equilibrium solution.

Finally, it remains to be proven that $\dot{V}$ is not identically zero along any solution of (4.10)-(4.13) other than the desired equilibrium solution. Clearly, $\dot{V} \equiv 0$ implies $\dot{\psi} = \dot{\theta} = v_z \equiv 0$. This, in turn, implies $\ddot{\psi} = \ddot{\theta} = \dot{v}_z = 0$, which implies $\psi = \theta = \tilde{v}_x = 0$. Therefore, the system is globally asymptotically stable at the desired equilibrium position.

After choosing suitable control parameter values r_1, r_2, r_3, r_4, l_1, and l_2, the nonlinear equations of motion can be integrated to simulate the system response. It is expected that, even when supplied with a large base-body angle initial condition, the Lyapunov controller will demonstrate superior performance in relation to its linearized counterparts developed in Chapter 3. Figures 5.13 and 5.14 illustrate this controller's

performance.

Chapter 5 will present the spacecraft parameters, gains, and simulated results of all the controllers developed in this research.

Chapter 5

Simulations

5.1 Introduction

The linear and nonlinear control methodologies discussed in Chapters 3 and 4 are implemented here for a theoretical spacecraft. The physical parameters of the craft, as well as the controller gain and weighting values are provided for each case.

The spacecraft characteristics are, for each controller:

Parameter	Value	Units
m	100	kg
I	30	$kg \ \ m^2$
m_f	20	kg
I_f	10	$kg \cdot m^2$
a	0.2	m
b	0.25	m
F	100	N
ϵ	0.1	$\frac{kg\,m^2}{s}$

Table 5.1: Physical spacecraft parameters.

The initial conditions are, for each controller:

Initial State	Value	Units
θ_o	2	deg
$\dot{\theta}_o$	0	$\frac{deg}{s}$
ψ_o	0	deg
$\dot{\psi}_o$	0	$\frac{deg}{s}$
v_{xo}	10000	$\frac{m}{s}$
v_{zo}	0	$\frac{m}{s}$

Table 5 2 Spacecraft initial conditions

5.2 Generalized Filter

5.2.1 Torquer Control

The controller gains for the generalized filter acting on an onboard torquer are

Gain	Value
K_p	0 1
K_d	1
g_1	1
g_2	1

Table 5 3 Gains for a generalized filter with torquer

The linear coefficients for the torquer model are

Coefficient	Value	Units
α_1	0 9219	1
ω_1	0 5590	$\frac{rad}{s}$
ζ_1	0 0084	1

Table 5 4 Linear coefficients for a generalized filter with torquer

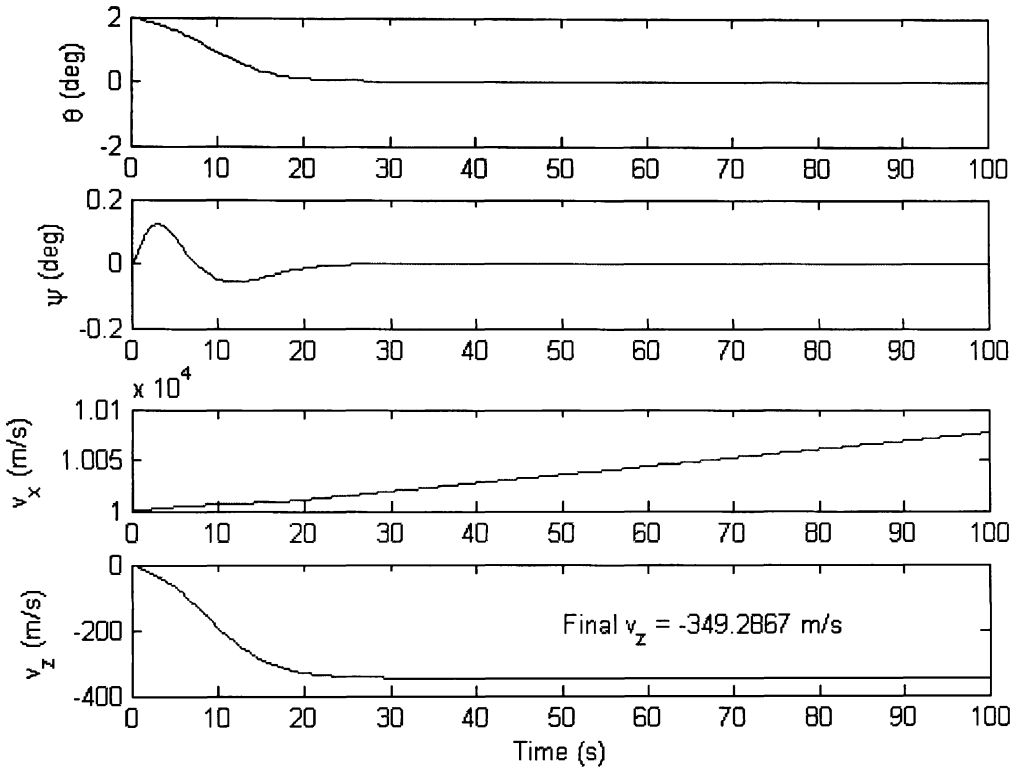

Figure 5.1: Momentum wheel controlled s/c state variables (PD controller with generalized filter).

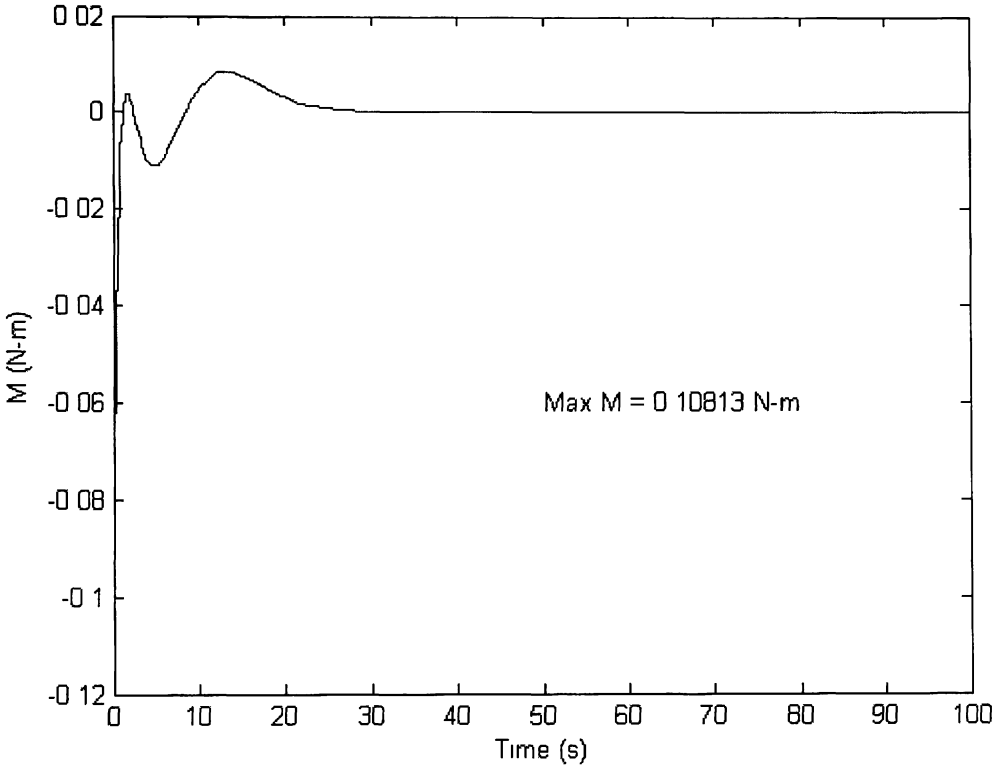

Figure 5.2: Momentum wheel torque (PD controller with generalized filter)

5.2.2 Side-Thruster Control

The controller gains for the generalized filter controller acting on a lateral thrusters are

Gain	Value
K_p	0 1
K_d	1
g_1	1
g_2	1

Table 5 5 Gains for a generalized filter with thrusters

The linear coefficients for the side-thruster model are

Coefficient	Value	Units
α_2	3 4000	1
ω_2	0 5774	$\frac{rad}{s}$
ζ_2	0 0017	1

Table 5 6 Linear coefficients for a generalized filter with side-thrusters

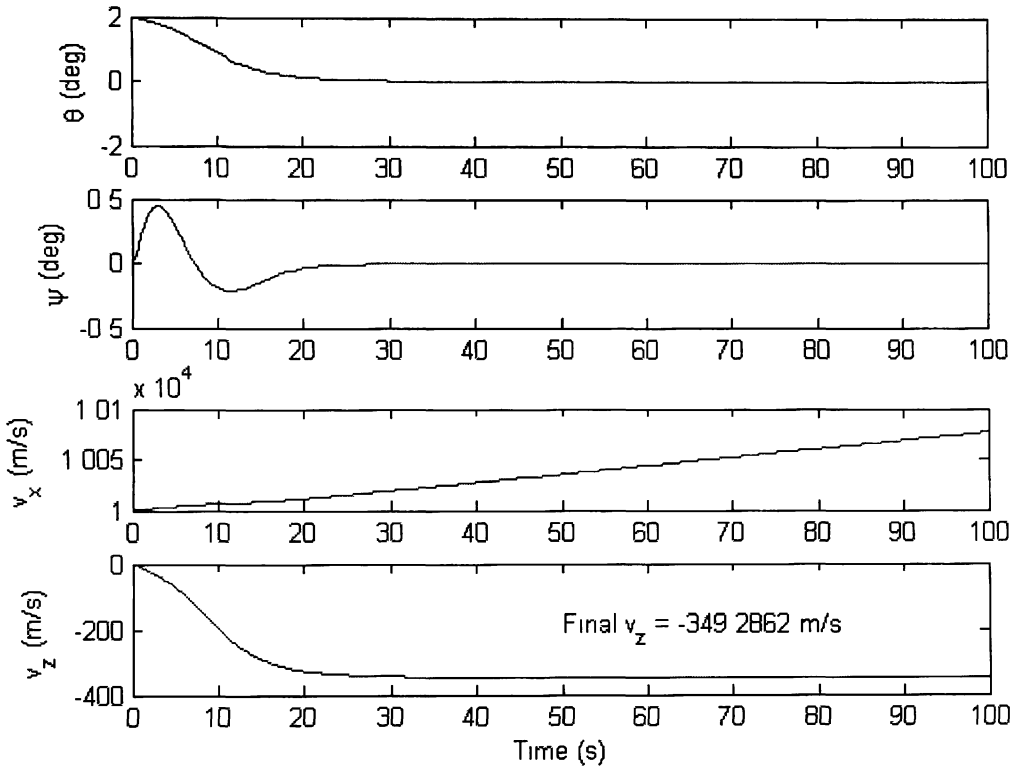

Figure 5.3: Side-thruster controlled s/c state variables (PD controller with generalized filter).

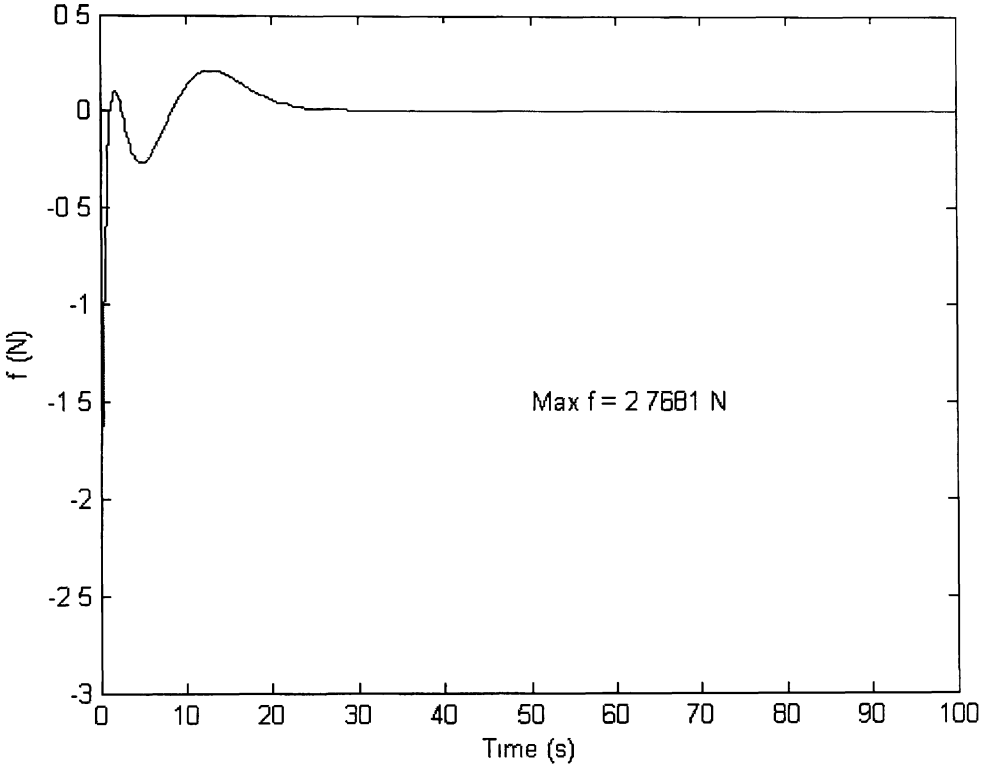

Figure 5.4: Side-thruster force (PD controller with generalized filter).

5.2.3 2-Phase Control

The controller gains for the two-phase generalized filter controller are:

Gain	Value
K_p	0.1
K_d	1
K_{vz}	0.03
g_1	1
g_2	1
h_1	1
h_2	1
λ	10

Table 5.7: Gains for a two-phase generalized filter

The linear coefficients for the two-phase generalized filter controller are:

Coefficient	Value	Units
α_1	0.9219	1
ω_1	0.5590	$\frac{rad}{s}$
ζ_1	0.0084	1

Table 5.8: Linear coefficients for a two-phase generalized filter (phase-one).

Coefficient	Value	Units
α_{vz}	0.3704	1
ω_{vz}	0.5556	$\frac{rad}{s}$
ζ_{vz}	0.0083	1

Table 5.9: Linear coefficients for a two-phase generalized filter (phase-two).

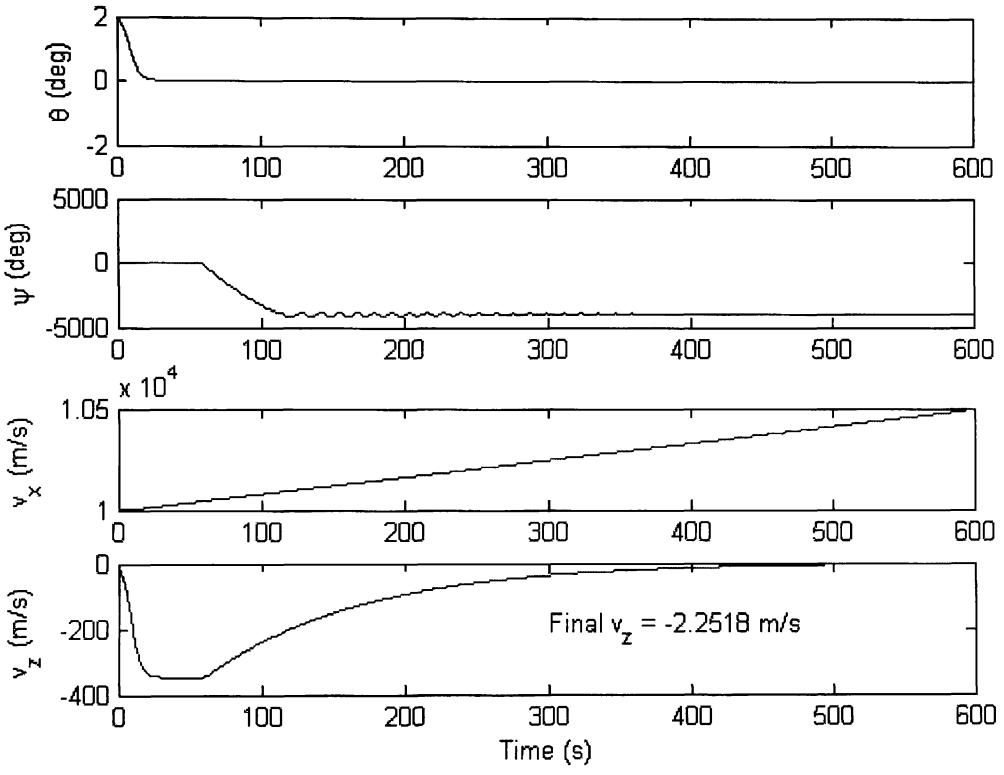

Figure 5.5: State variables (two-phase generalized filter controller).

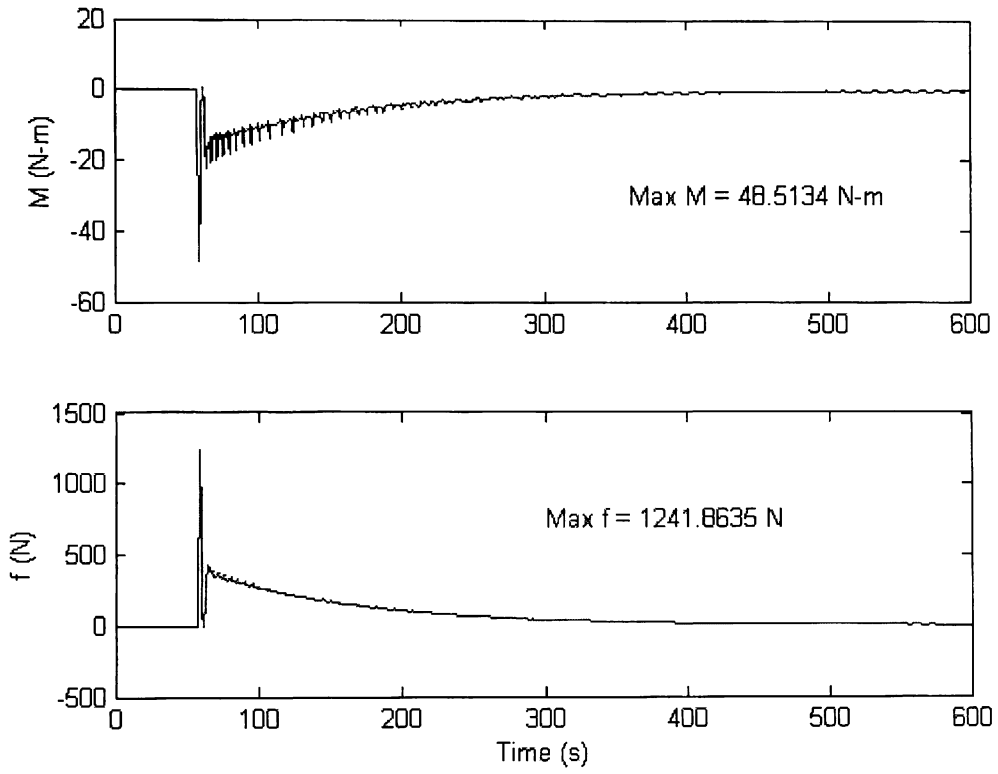

Figure 5.6: Torque and side-thrust (two-phase generalized filter controller).

5.3 Linear Quadratic Regulator

5.3.1 Torquer Control

The weighting matrices for the LQR acting on the onboard torquer are:

$$\boldsymbol{Q} = \begin{bmatrix} 1 & 0 & 0 & 0 \\ 0 & 10 & 0 & 0 \\ 0 & 0 & 1 & 0 \\ 0 & 0 & 0 & 10 \end{bmatrix}, \qquad \boldsymbol{R} = [0.1]$$

The linear coefficients for the torquer model are:

Coefficient	Value	Units
α_1	0.9219	1
ω_1	0.5590	$\frac{rad}{s}$
ζ_1	0.0084	1

Table 5.10: Linear coefficients for the LQR with torquer.

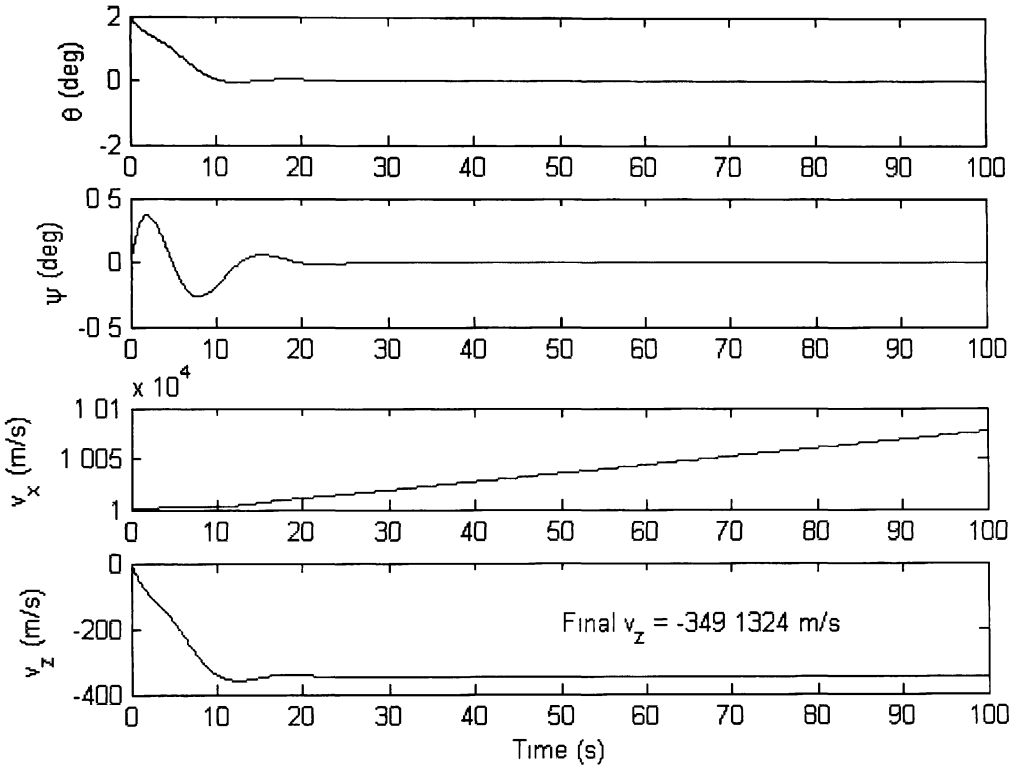

Figure 5.7: State variables for momentum wheel controlled spacecraft (LQR controller).

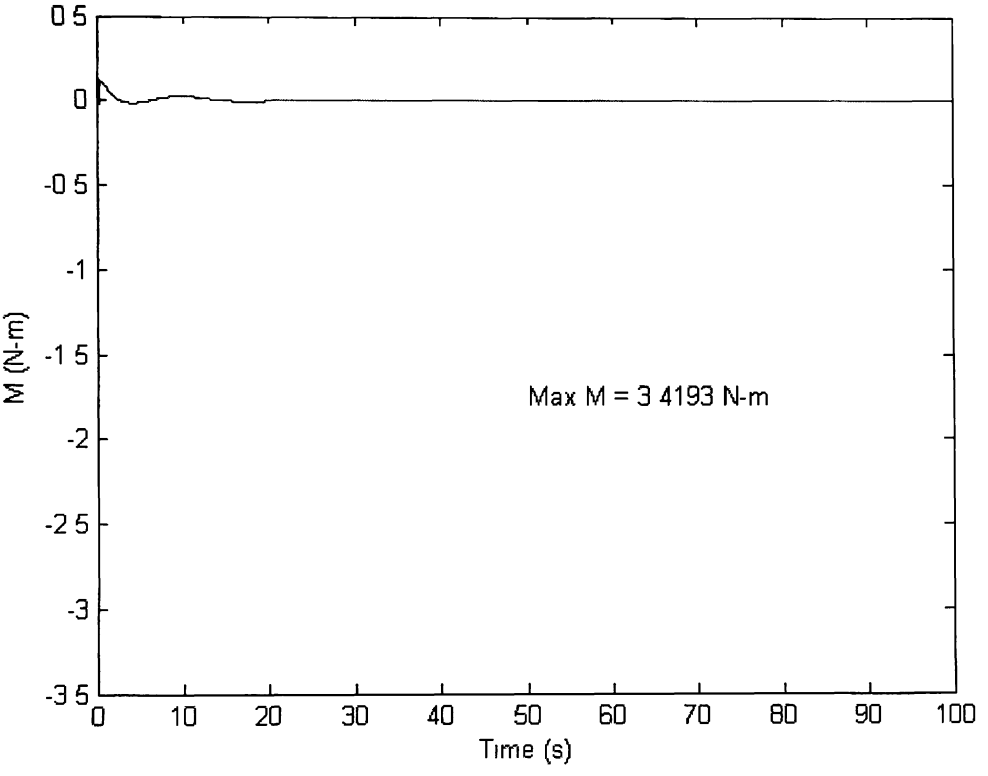

Figure 5.8: Momentum wheel torque (LQR controller).

5.3.2 Side-Thruster Control

The weighting matrices for the LQR acting on the lateral thrusters are:

$$\boldsymbol{Q} = \begin{bmatrix} 1 & 0 & 0 & 0 \\ 0 & 10 & 0 & 0 \\ 0 & 0 & 1 & 0 \\ 0 & 0 & 0 & 10 \end{bmatrix}, \qquad \boldsymbol{R} = [100]$$

The linear coefficients for the side-thruster model are:

Coefficient	Value	Units
α_2	3.4000	1
ω_2	0.5774	$\frac{rad}{s}$
ζ_2	0.0017	1

Table 5.11: Linear coefficients for the LQR with side-thrusters.

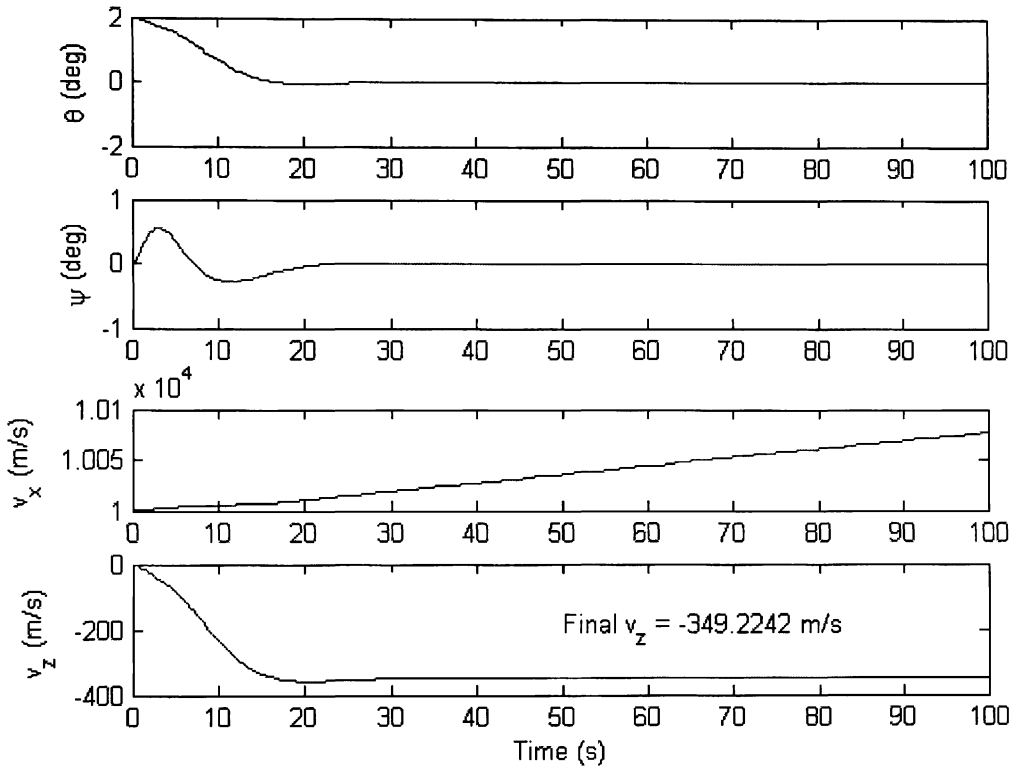

Figure 5.9: State variables for side-thruster controlled spacecraft (LQR controller).

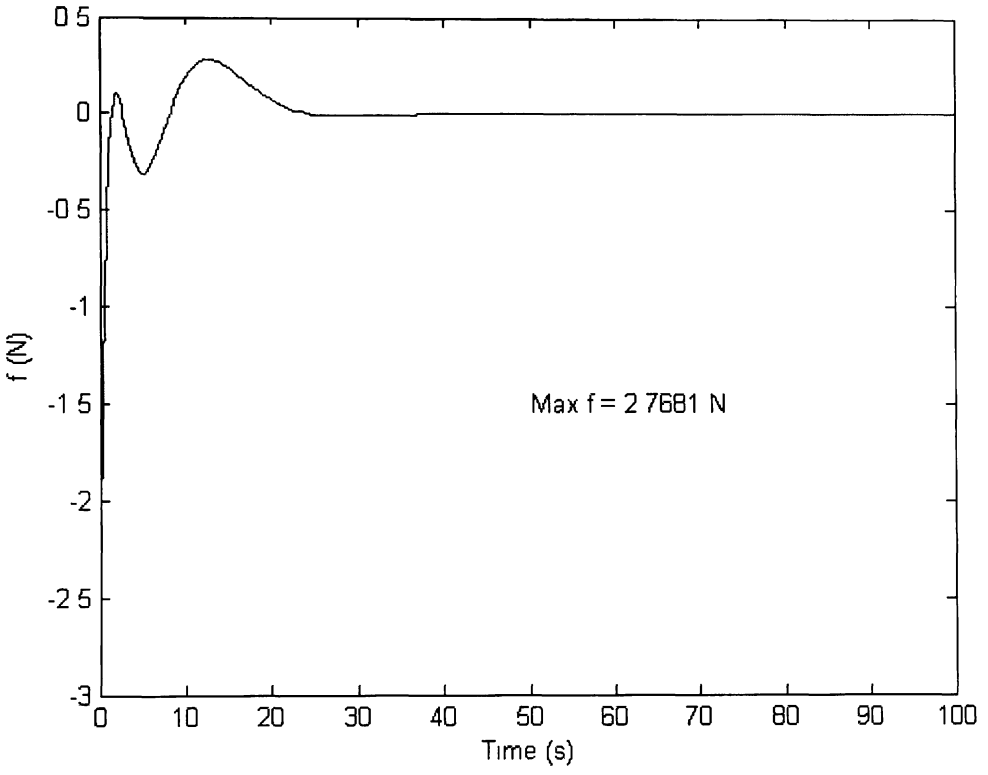

Figure 5.10: Side-thruster force (LQR controller).

5.3.3 2-Phase Control

The weighting matrices for the two-phase Linear Quadratic Regulator are

$$\boldsymbol{Q} = \begin{bmatrix} 1 & 0 & 0 & 0 \\ 0 & 10 & 0 & 0 \\ 0 & 0 & 1 & 0 \\ 0 & 0 & 0 & 10 \end{bmatrix}, \qquad \boldsymbol{R} = [\,1]$$

$$\boldsymbol{Q}_{vz} = \begin{bmatrix} 1 & 0 & 0 \\ 0 & 1 & 0 \\ 0 & 0 & 1 \end{bmatrix}, \qquad \boldsymbol{R}_{vz} = [10000]\,, \qquad \lambda = 1$$

The linear coefficients for the two-phase generalized filter controller are

Coefficient	Value	Units
α_1	0 9219	1
ω_1	0 5590	$\frac{rad}{s}$
ζ_1	0 0084	1

Table 5 12 Linear coefficients for a two-phase linear quadratic regulator (phase-one)

Coefficient	Value	Units
α_{vz}	0 3704	1
ω_{vz}	0 5556	$\frac{rad}{s}$
ζ_{vz}	0 0083	1

Table 5 13 Linear coefficients for a two-phase linear quadratic regulator (phase-two)

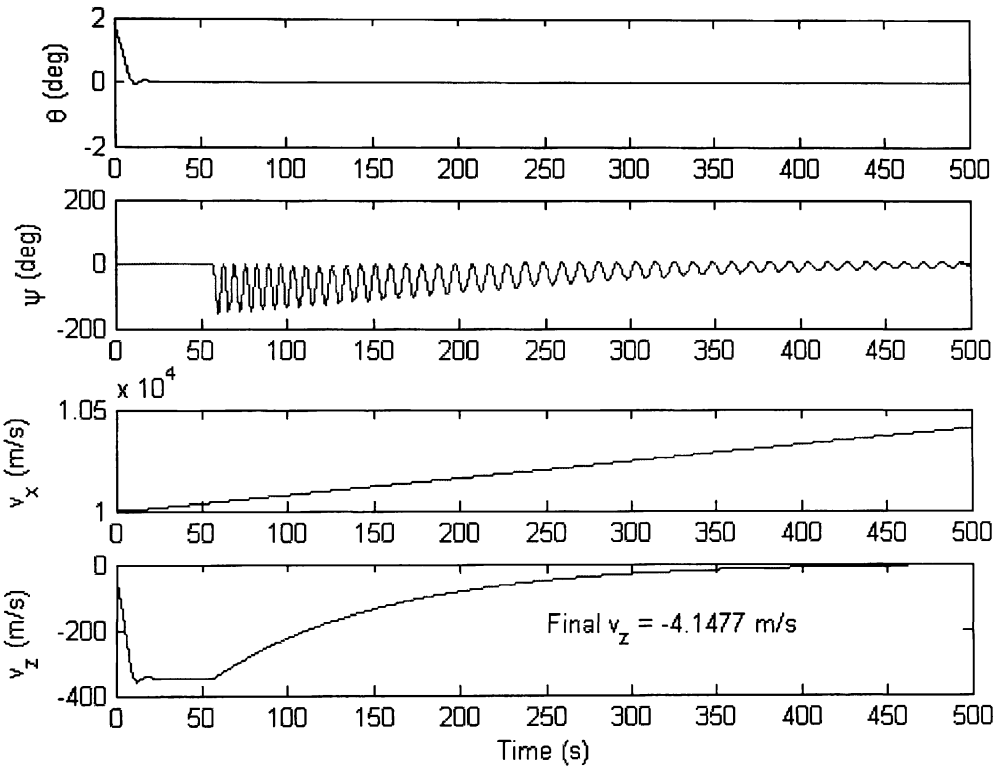

Figure 5.11: State variables (two-phase LQR controller).

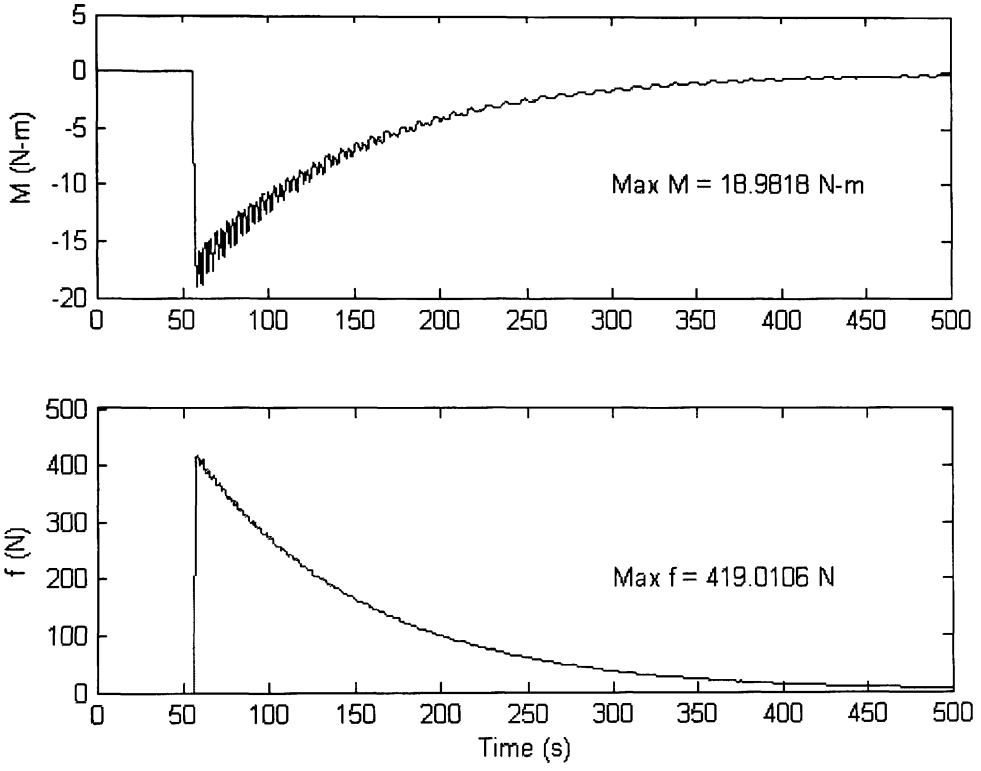

Figure 5.12: Torque and side-thruster force (two-phase LQR controller).

5.4 Lyapunov Controller

The controller gains for the Lyapunov controller acting on both the torquer and the thrusters are:

Gain	Value
r_1	1×10^{-7}
r_2	10
r_3	1000
r_4	1×10^{-7}
l_1	1×10^{5}
l_2	1

Table 5.14: Gains for a Lyapunov controller

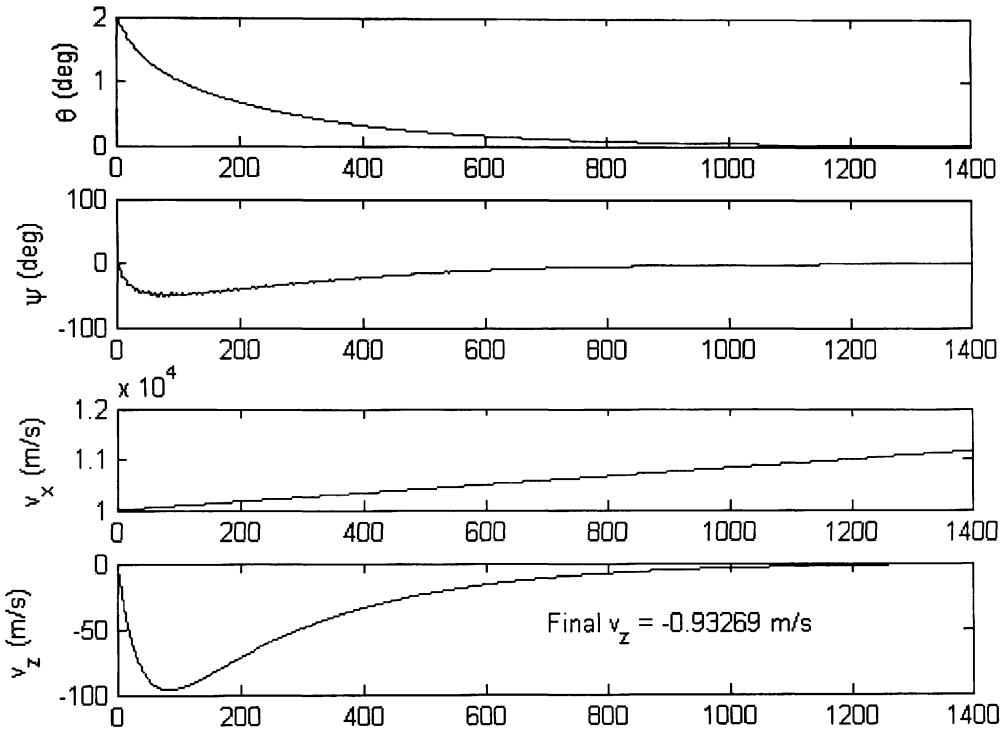

Figure 5.13: State variables (Lyapunov-based controller).

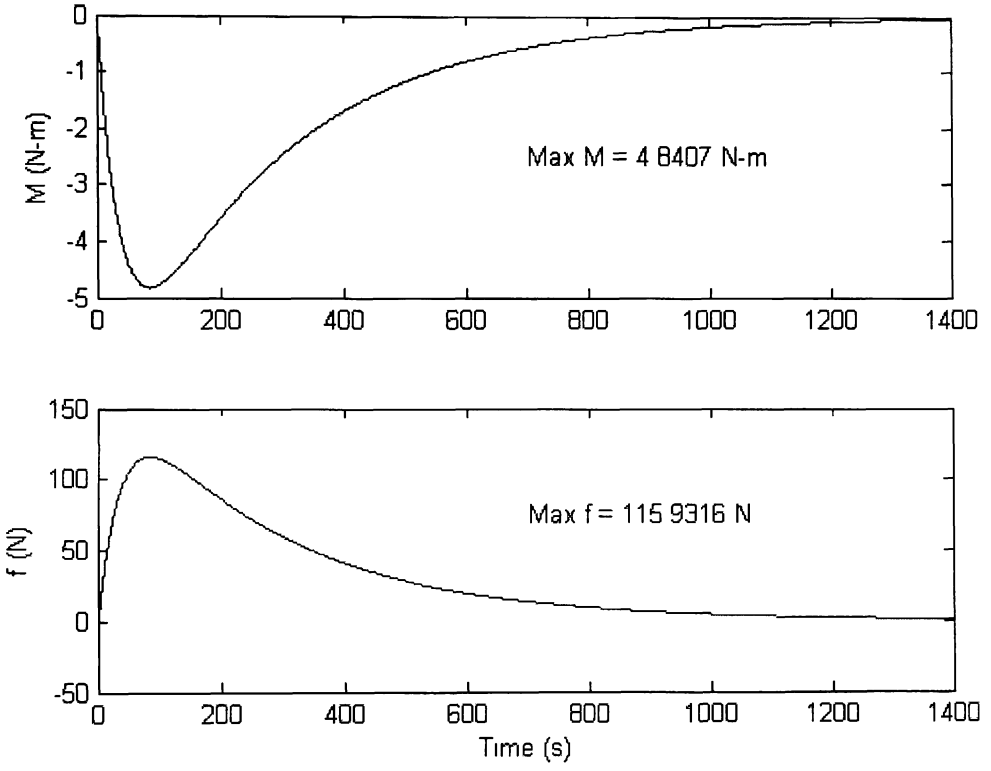

Figure 5.14: Torque and side-thruster force (Lyapunov-based controller).

To demonstrate the ability of Lyapunov's second method to stabilize a nonlinear system, the Lyapunov controller simulation was run a second time for an aggressive maneuver of 15 degrees.

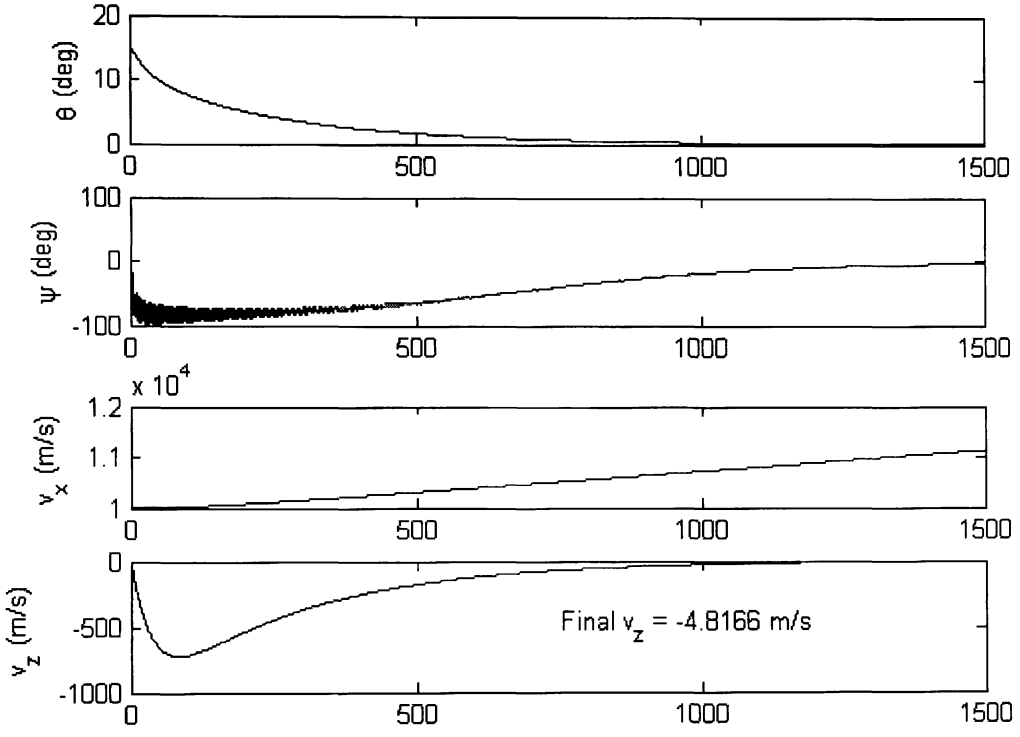

Figure 5.15: State variables (Lyapunov-based controller-aggressive maneuver).

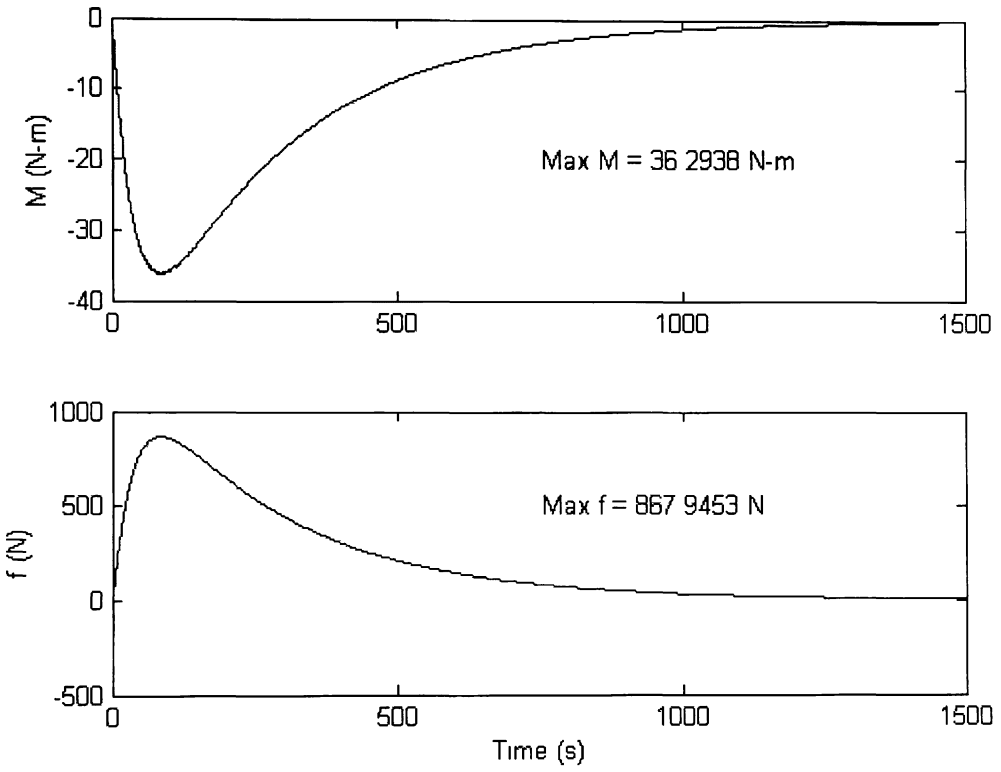

Figure 5.16: Torque and side-thruster force (Lyapunov-based controller-aggressive maneuver).

Chapter 6

Conclusions and Future Research

6.1 Introduction

This chapter discusses the results of the exploration of controller types discussed in this thesis. State output of a given controller/actuator combination is compared to that of other controllers and actuators.

6.2 PD Controller with Generalized Filter

6.2.1 Torquer Only

Figure 5.1 shows the vehicle state, $(x_1, x_3, x_5, x_6) = (\theta, \psi, v_x, v_z)$ for the simulation timespan of 100 seconds. The orientation angles of the the base-body and the slosh mass approach the desired state within 30 seconds. The axial velocity v_x increases linearly under the influence of the main engine as expected. The transverse velocity, v_z, reaches steady-state roughly 350 $\frac{m}{s}$ below the initial velocity. This final v_z offset is a product of the inability of the controller to drive all state variables to equilibrium with a single actuator. Figure 5.2 displays the torque provided by the control

momentum wheel (or other onboard torquer). The maximum torque supplied (0.11 N-m) is well within the range of available hardware.

6.2.2 Thruster Only

Pitch-control with the side-thrusters produces Figure 5.3. The pitch angle ouput and transverse velocity are virtually identical to the torquer-only case, and the axial velocity remains well-behaved. The slosh angle, ψ, experiences a maximum amplitude four-times greater than the torquer case. The side-thruster force is shown in Figure 5.4. Maximum thruster output (2.8 N) is achievable with current small-satellite maneuvering systems.

6.2.3 2-Phase Control

The two-phase generalized filter controller is successful is driving all spacecraft states to the desired values within the simulation time-frame (Figure 5.5). Pitch control is, again, identical to the torquer-only case, since phase-one utilizes the same controller gains. The specified error condition (10^{-6}) is achieved at $t = 59$ seconds, at which time the thrusters fire to suppress any residual lateral velocity (evident in the sudden "kick" of the slosh-angle), and the momentum wheel acts to maintain pitch. The entire system stabilizes in approximately 600 seconds. It is noted that the final slosh-angle is 3960 deg - an equilibrium state when complete revolutions are allowed. Figure 5.6 reveals the actuator behaviors during both phases. At switch time the momentum wheel torque peaks at 49 N-m, and the thruster output peaks at 1240 N. Although the simulation reveals a successful control concept, the side-thruster force is not practical for a spacecraft of this size. These maximum values may be adjusted by altering the controller gains, or inserting maximum limit conditions in the simulation coding (see

Section 6.5).

6.3 Linear Quadratic Regulator

6.3.1 Torquer Only

The Linear Quadratic Regulator acting on the onboard torquer produces the state behavior of Figure 5.7. The pitch angle stabilizes to zero and the lateral velocity achieves its final state in roughly two-thirds the time of the corresponding filter/torquer combination. The trade-offs are seen in the maximum pitch-angle (three-times that of the filter), and the torquer output of Figure 5.8. Although this actuator maximum output is thirty-times greater than that of the filter, the maximum required torque is still within the operating range of momentum wheels and control moment gyros.

6.3.2 Side-Thruster Only

Figure 5.9 demonstrates the performance of the LQR/thruster combination. The side-thruster controllers continue to produce larger maximum slosh-angles, as ψ peaks nearly twice as high as in the LQR/torquer case. The response time and actuator output (Figure 5.10) are similar to the generalized filter controller.

6.3.3 2-Phase Control

Figure 5.11 reveals that the pitch and slosh angles achieve their desired states in the LQR first-phase at $t = 57$ seconds. While switching, the thruster re-introduces a slosh oscillation with an amplitude greater than that of the two-phase filter controller, but damps to zero without total revolutions of the slosh-mass. The system (including v_z) stabilizes in nearly the same amount of time. The maximum side-thruster force and

momentum wheel torque is less than half that of the filter case as seen in Figure 5.12.

6.4 Lyapunov Controller

The performance of the nonlinear controller using Lyapunov's direct method is shown in Figure 5.13. The pitch-angle achieves the desired state in approximately 1500 seconds - a greater time-span than the linear controllers. Also, the slosh-angle maximum is among the highest of all the controllers. However, unlike the previous controllers, the Lyapunov controller lateral velocity is driven to the equilibrium state with the base-body and pitch angles simultaneously, eliminating the need for two-phase control. Also, the maximum v_z is less than 100 $\frac{m}{s}$. In addition, this is accomplished with a maximum torque and side-thruster force far less than either of the two-phase controllers (Figure 5.14).

An aggressive maneuver of $\Delta\theta = 15$ degrees is performed by the Lyapunov controller in Figure 5.15. That Lyapunov's direct method allows stability analysis while retaining nonlinear terms allows the Lyapunov controller to succeed where the linear controllers would not. All state variables are driven to the desired positions within approximately the same amount of time as the "tame" case. Figure 5.16 shows that the torquer action peaks at 38 N, and the side-thruster force at 870 N. Again, although these actuator requirements are impractical for the small spacecraft considered, they may be adjusted via the controller gains at the expense of the response time.

6.5 Future Research

The course of this research revealed the richness of the propellant slosh problem. Among the many avenues considered for future exploration include:

- **Controller constraints and efficiency**. Although the gains were adjusted to produce desirable responses with reasonable torques and thruster forces, a comprehensive investigation of methods to limit maximum actuator outputs would better quantify the relative strengths and weaknesses of the linear and nonlinear controllers.

- **Thrust vector control**. Many spacecraft (especially launch vehicles) lack torquers or lateral thrusters during aggresive maneuvers. Adaptation of the system model and control laws to vectored thrust systems would expand the usefullness of these results to other spacecraft types.

- **Multiple tanks**. Most spacecraft main engines utilize bipropellants consisting of a liquid fuel and oxidizer. The practicality of extending the techniques found here to two or more tanks should be explored.

- **Gravity**. The system model found in this thesis considers only the field-free space case, where gravitational potential can be neglected. Pitch-up maneuvers in the near-earth environment must take the gravitational forces into account if they are to remain robust. Of course, this course of development would also be necessary for launch vehicles.

- **3-D**. Planar pitch-maneuvers are addressed in this thesis. The expansion of these techniques into three-dimensional geometry would further promote nonlinear control theory's role spacecraft maneuvers.

- **Higher order slosh modes**. The most prevalent, first mode of oscillation provides the general picture of the behavior of fuel slosh as a pendulum mass. In reality, higher frequency oscillations are superimposed that, although less energetic, may affect the translation of the theoretical model into reality. Possible

modifications include a multiple pendulum or multiple spring mass approach.

- **Robustness issues**. Although many of the spacecraft parameters are actually time varying, they are held fixed for analysis purposes. However, gain scheduling may be needed to compensate for large variations that occur in spacecraft mass and inertia properties as propellants are depleted.

Bibliography

[1] M. J. Sidi. *Spacecraft Dynamics and Control*, chapter 10. Cambridge Aerospace Series. Cambridge University Press, 1997.

[2] NASA. *Slosh Suppression*, May 1969. NASA SP-8031.

[3] K. C. Biswal, S. K. Bhattacharyya, and P. K. Sinha. "Dynamic Characteristics of Liquid Filled Rectangular Tank with Baffles" *IE (I) Journal-CV*, 84, August 2003.

[4] R. Venugopal and D. S. Bernstein. "State Space Modeling and Active Control of Slosh" In *International Conference on Control Applications*, number WP08 3:15, pages 1072–1077, September 1996.

[5] C. Hubert. "Behavior of Spinning Space Vehicles with Onboard Liquids" Hubert Astronautics, Inc. NASA/KSC contract NAS10-02016.

[6] C. Hubert. "Design and Flight Performance of a System for Rapid Attitude Maneuvers by a Spinning Vehicle". In *27th Annual AAS Guidance and Control Conference*, number AAS 04-078, Breckenridge, Colorado, February 2004. American Astronautical Society.

[7] T. R. Blackburn and D. R. Vaughan. "Application of Linear Optimal Control

and Filtering Theory to the Saturn V Launch Vehicle". *IEEE Transactions on Automatic Control*, AC-16(6):799–806, December 1971.

[8] J. Freudenberg and B. Morton. "Robust Control of a Booster Vehicle Using H^∞ and SSV Techniques" In *31st IEEE Conference on Decision and Control*, pages 2448–2453, December 1992.

[9] L. D. Peterson, E. F. Crawley, and R. J. Hansman. "Nonlinear Fluid Slosh Coupled to the Dynamics of a Spacecraft" *AIAA Journal*, 27(9):1230–1240, 1989.

[10] A. E. Bryson. *Control of Spacecraft and Aircraft.* Princeton University Press, 1994.

[11] B. Wie. *Space Vehicle Dynamics and Control.* AIAA, 1998.

[12] J. M. Adler, M. S. Lee, and J. D. Saugen. "Adaptive Control of Propellant Slosh for Launch Vehicles" *SPIE Sensors and Sensor Integration*, 1480:11–22, 1991.

[13] J. T. Feddema, C. R. Dohrmann, G. G. Parker, R. D. Robinett, V. J. Romero, and D. J. Schmitt. "Control for Slosh-Free Motion of an Open Container" *IEEE Control Systems Magazine*, pages 29–36, February 1997.

[14] M. Grundelius and B. Bernhardsson. "Motion Control of Open Containers with Slosh Constraints", 1999. Department of Automatic Control, Lund Institute of Technology, Lund, Sweden.

[15] M. Grundelius. "Iterative Optimal Control of Liquid Slosh in an Industrial Packaging Machine" In *Proceedings of the 39th IEEE Conference on Decision and Control*, pages 3427–3432, December 2000.

[16] M. Grundelius and B. Bernhardsson. "Control of Liquid Slosh in an Industrial Packaging Machine". In *Proceedings of the 1999 IEEE International Conference on Control Applications*, pages 1654–1659, August 1999.

[17] K. Yano, T. Toda, and K. Terashima. "Sloshing Suppression Control of Automatic Pouring Robot by Hybrid Shape Approach" In *Proceedings of the 40th IEEE Conference on Decision and Control*, pages 1328–1333, December 2001.

[18] K. Yano, S. Higashikawa, and K. Terashima. "Liquid Container Transfer Control on 3D Transfer Path by Hybrid Shaped Approach" In *Proceedings of the 2001 IEEE International Conference on Control Applications*, pages 1168–1173, September 2001.

[19] K. Yano and K. Terashima. "Robust Liquid Container Transfer Control for Complete Sloshing Suppression". *IEEE Transactions on Control Systems Technology*, 9(3):483–493, May 2001.

[20] K. Terashima and G. Schmidt "Motion Control of a Cart-Based Container Considering Suppression of Liquid Oscillations" In *Proceedings of the IEEE International Symposium on Industrial Electronics*, pages 275–280, May 1994.

[21] D. H. Kim and J W. Choi. "Attitude Controller Design for a Launch Vehicle with Fuel-Slosh". *SICE*, (214 A-4):235–240, July 2000.

[22] S. Cho, N. H. McClamroch, and M. Reyhanoglu. "Dynamics of Multibody Vehicles and their Formulation as Nonlinear Control Systems". In *Proceedings of American Control Conference*, pages 3908–3912, June 2000.

[23] L. Meirovitch and M. K. Kwak. "State Equations for a Spacecraft with Maneuvering Flexible Appendages in Terms of Quasi-Coordinates". *Applied Mechanics Reviews*, 42(11):161–170, Nov 1989.

[24] J. B. Marion and S. T. Thornton. *Classical Dynamics*, chapter 3. Harcourt Brace & Company, 4th edition, 1995.

[25] K. Ogata. *Modern Control Engineering*. Prentice Hall, 3rd edition, 1997.

[26] H.K. Khalil. *Nonlinear Systems*. Prentice-Hall, 3rd edition, 2002.

[27] M. Reyhanoglu. "Maneuvering Control Problems for a Spacecraft with Unactuated Fuel Slosh Dynamcis" In *Proceedings of the IEEE Conference on Control Applications*, pages 695–699, June 2003.

[28] S. Cho, N. H. McClamroch, and M Reyhanoglu. "Feedback Control of a Space Vehicle with Unactuated Fuel Slosh Dynamics" In *Proceedings of AIAA Guidance, Navigation, and Control Conference*, number AIAA 2000-4046, 2000